Influence of fuel sulfur on the composition of aircraft exhaust plumes: The experiments SULFUR 1–7

U. Schumann,[1] F. Arnold,[2] R. Busen,[1] J. Curtius,[2,3] B. Kärcher,[1] A. Kiendler,[2] A. Petzold,[1] H. Schlager,[1] F. Schröder,[1] and K.-H. Wohlfrom[2]

[1]   The series of SULFUR experiments was performed to determine the aerosol particle and contrail formation properties of aircraft exhaust plumes for different fuel sulfur contents (FSC, from 2 to 5500 µg/g), flight conditions, and aircraft (ATTAS, A310, A340, B707, B747, B737, DC8, DC10). This paper describes the experiments and summarizes the results obtained, including new results from SULFUR 7. The conversion fraction ε of fuel sulfur to sulfuric acid is measured in the range 0.34 to 4.5% for an older (Mk501) and 3.3 ± 1.8% for a modern engine (CFM56-3B1). For low FSC, ε is considerably smaller than what is implied by the volume of volatile particles in the exhaust. For FSC $\geq$ 100 µg/g and ε as measured, sulfuric acid is the most important precursor of volatile aerosols formed in aircraft exhaust plumes of modern engines. The aerosol measured in the plumes of various aircraft and models suggests ε to vary between 0.5 and 10% depending on the engine and its state of operation. The number of particles emitted from various subsonic aircraft engines or formed in the exhaust plume per unit mass of burned fuel varies from 2×10^{14} to 3×10^{15} kg^{-1} for nonvolatile particles (mainly black carbon or soot) and is of order 2×10^{17} kg^{-1} for volatile particles >1.5 nm at plume ages of a few seconds. Chemiions (CIs) formed in kerosene combustion are found to be quite abundant and massive. CIs contain sulfur-bearing molecules and organic matter. The concentration of CIs at engine exit is nearly 10^9 cm^{-3}. Positive and negative CIs are found with masses partially exceeding 8500 atomic mass units. The measured number of volatile particles cannot be explained with binary homogeneous nucleation theory but is strongly related to the number of CIs. The number of ice particles in young contrails is close to the number of soot particles at low FSC and increases with increasing FSC. Changes in soot particles and FSC have little impact on the threshold temperature for contrail formation (less than 0.4 K).   *INDEX TERMS:* 0305 Atmospheric Composition and Structure: Aerosols and particles (0345, 4801); 0320 Atmospheric Composition and Structure: Cloud physics and chemistry; 0345 Atmospheric Composition and Structure: Pollution—urban and regional (0305); *KEYWORDS:* chemiion, sulfur, soot, contrail, aircraft, emission

1. Introduction

[2]   A series of experiments (SULFUR 1–7, abbreviated as S1–S7) was performed in the years from 1994 to 1999 in order to determine the particle and contrail formation properties of aircraft exhaust plumes for different fuel sulfur content (FSC) and atmospheric conditions. This paper describes the series of experiments and summarizes the results obtained. In particular, the paper discusses the evolution of our understanding of particle formation and contrails as obtained during the course of these and related experiments.

[3]   Particle and contrail formation in aircraft exhaust plumes as a function of FSC is of importance for air composition and climate [*Brasseur et al.*, 1998; *Fahey et al.*, 1999; *Schumann et al.*, 2001]. Before the first SULFUR experiment in 1994, it was hypothesized that sulfuric acid in aircraft exhaust plumes plays a strong role with respect to the number of volatile particles formed from aircraft, "activation" of soot particles as cloud condensation nuclei, and possibly "passivation" of soot for heterogeneous chemistry. These effects are important for contrail formation and air composition with possible impact on aerosols, cloudiness and climate [*Turco et al.*, 1980; *Hofmann*, 1991; *Reiner and Arnold*, 1993; *Schumann*, 1994; *Arnold et al.*, 1994]. In young exhaust plumes many small condensation nuclei (CN) were measured, but at nontypical ambient conditions (2600 m altitude, 11°C) [*Pitchford et al.*, 1991]. Soot particles were noted to hydrate when formed from fuel with high sulfur content but do not hydrate

[1]Institut für Physik der Atmosphäre, Deutsches Zentrum für Luft- und Raumfahrt, Oberpfaffenhofen, Wessling, Germany.
[2]Bereich Atmosphärenphysik, Max-Planck-Institut für Kernphysik, Heidelberg, Germany.
[3]Now at Institute for Atmospheric Physics, Johannes Gutenberg University Mainz, Mainz, Germany.

otherwise [*Hallett et al.*, 1990; *Whitefield et al.*, 1993]. It was assumed that most of the fuel sulfur is burned to sulfur dioxide (SO_2) in the combustion chamber of the engine. A fraction is oxidized by reactions with co-emitted hydroxyl radicals (OH) and water to S^{VI} in form of sulfur trioxide (SO_3) and sulfuric acid (H_2SO_4) [*Miake-Lye et al.*, 1993; *Reiner and Arnold*, 1993, 1994; *Kolb et al.*, 1994]. The sulfuric acid was assumed to form liquid volatile particles by binary homogeneous nucleation [*Hofmann and Rosen*, 1978], to interact with soot [*Zhao and Turco*, 1995], and to affect contrail formation [*Kärcher et al.*, 1995]. Standard emission measurements for aircraft engines provide the smoke number (a measure for the optical blackening of a filter exposed to a given volume of exhaust gases), which may be converted with some assumptions to soot mass emissions [*Petzold et al.*, 1999], but little was known on the number, sizes and hydration properties of aviation soot from cruising aircraft [*Pitchford et al.*, 1991]. Measurements at ground behind a jet engine by *Frenzel and Arnold* [1994] showed that aircraft engines emit chemiions (CIs) formed by radical-radical reactions during the combustion process and indicated the presence of gaseous H_2SO_4. They inferred a conversion fraction ε of fuel sulfur to sulfuric acid of more than 0.4%, suggested that atomic oxygen forming during the combustion may contribute to oxidizing sulfur dioxide in addition to OH, and proposed that CIs may act as condensation nuclei for particle formation.

[4] In October 1994, particle measurements in the exhaust plume of a Concorde supersonic aircraft with the stratospheric research aircraft ER-2 revealed far larger number concentrations of small particles within aircraft exhaust plumes than expected before [*Fahey et al.*, 1995]. The emission index of non-volatile particles was derived from measurements with a condensation particle counter (CPC) [*Wilson et al.*, 1983] during three short (<20 s) plume penetrations with significant CO_2 concentration increases defining dilution at plume ages of 16–58 min. To avoid saturation effects, the ratio between total and nonvolatile particle concentration was derived from weaker plume events. From the data the amount of sulfuric acid formed in the exhaust was estimated assuming that the volatile particles were composed of sulfuric acid and water only and that the expected cutoff size (~9 nm) of the CPCs was close to the volume mean diameter of the particles. This way, a very large conversion fraction ε was derived, larger than 12%, possibly exceeding 45%. The conversion fraction predicted by models assuming zero conversion at engine exit was of order 1% [*Miake-Lye et al.*, 1994; see also *Kärcher et al.*, 1995, 1996a; *Brown et al.*, 1996a; *Tremmel et al.*, 1998]. Concurrent measurements of OH formed in the plume suggested that less than 2% of SO_2 is oxidized by OH via gas-phase reactions in the Concorde plume [*Hanisco et al.*, 1997]. New models were set up to compute the sulfur oxidation within engine combustors and turbines [*Brown et al.*, 1996b]. The models suggested ε values up to 10% for the Concorde engine. Larger values could not be excluded in view of some measurements behind conventional gas turbines [*Hunter*, 1982; *Harris*, 1990; *Farago*, 1991].

[5] Large conversion fractions would have important consequences for the impact of aircraft on air chemistry [*Weisenstein et al.*, 1996] and on contrail formation [*Miake-Lye et al.*, 1994; *Kärcher et al.*, 1996b]. The classical criterion [*Appleman*, 1953] implies contrail formation when the plume reaches liquid saturation. Even for a modest amount of fuel sulfur to sulfuric acid conversion, very large number densities of sulfuric acid droplets were computed (more than 10^{11} cm^{-3} for 0.6% conversion fraction [*Miake-Lye et al.*, 1994]). With a high amount of soot and sulfuric acid in the exhaust plume, it was conceived possible that contrails form already when reaching ice saturation, i.e., at about 3 to 4 K (increasing with altitude) higher ambient temperature than if forming at liquid saturation, which could considerably extend the atmospheric region in which contrails form [*Miake-Lye et al.*, 1993; *Schumann*, 1996a].

[6] Hence the topic was of high interest with many open questions: How many soot particles are formed per mass unit of burned fuel and how large are these soot particles? How large is the conversion fraction ε of fuel sulfur to sulfuric acid? How many CIs are emitted and how important are CIs for particle formation? How many volatile particles are formed per mass of burned fuel? What is the impact of fuel sulfur on contrail formation? How important is the FSC for volatile aerosol formation, soot activation, and contrail ice crystal formation?

[7] Therefore the series of SULFUR experiments was initiated in December 1994. New questions arising from the results of the earlier experiments and new instrument developments led to the series of experiments to be described in this paper. Many of the results of the individual experiments have been published shortly after the experiments by various teams of authors, and these papers will be cited below, but none of them gives a full account for the series of experiments performed so far. This paper gives a synopsis of the experimental conditions and the results, and it describes the sequence of understanding obtained during the development of the research in this field. The discussion includes results from related measurements performed by our group within the Pollution From Aircraft Emissions in the North Atlantic Flight Corridor (POLINAT) projects [*Schumann et al.*, 2000a] with plume measurements behind several aircraft including the NASA DC8 [*Thompson et al.*, 2000]. Also included are results of the NASA Subsonic Aircraft Contrail and Cloud Effects Special Study (SUCCESS) [*Toon and Miake-Lye*, 1998] and a series of Subsonic Assessment Near-Field Interactions Field Experiments (SNIF, I–III) [*Hunton et al.*, 2000]. Moreover, we report results obtained at ground within this series of experiments and within related projects, including modeling performed during the Chemistry and Microphysics of Contrail Formation (CHEMICON) project [*Gleitsmann and Zellner*, 1999; *Tremmel and Schumann*, 1999; *Sorokin and Mirabel*, 2001; *Starik et al.*, 2002]. Additionally, new data are reported from the most recent SULFUR 7 experiment.

2. Experiments

[8] The series of SULFUR experiments, see Table 1, was initiated by Deutsches Zentrum für Luft- und Raumfahrt, Institut für Physik der Atmosphäre (DLR, IPA), and performed in close cooperation with partners, in particular with Max-Planck-Institut für Kernphysik (MPIK), Heidelberg, to

Table 1. Summary of SULFUR Experiments

Experiment[a]	Date	Aircraft Investigated	FSC; Left/Right, μg/g	Experimental Topics; Observation Platform	Publications Describing Experiment Results
1	13 December 1994	ATTAS	2 ± 0.7/250 ± 17	visual check of threshold conditions for contrail onset; Lufthansa Piper Cheyenne	*Busen and Schumann* [1995]
2	22 March 1995	ATTAS	170 ± 10/5500 ± 100	first microphysical measurements; DLR Falcon	*Schumann et al.* [1996], *Gierens and Schumann* [1996]
3	13 July 1995	ATTAS	212/2800 ± 160	emissions at engine exit; ground	*Arnold et al.* [1998a]
4	8–15 March 1996	ATTAS; A310-300	6 ± 2/2830 ± 280; 850 ± 10/ 2700 ± 200	variation of aircraft, FSC and first near-field measurements in exhaust plumes and contrails; Falcon and ground behind ATTAS	*Petzold et al.* [1997], *Petzold and Schröder* [1998], *Petzold and Döpelheuer* [1998], *Arnold et al.* [1998b], *Schröder et al.* [2000a]
5	14–18 April 1997	ATTAS	22 ± 2/2700 ± 350	first measurements of sulfuric acid, chemiions, volatile and non-volatile aerosols within and outside contrails, soot impact on ice particles, emissions of hydrocarbons and carbon monoxide; Falcon and ground	*Curtius et al.* [1998], *Schröder et al.* [1998], *Arnold et al.* [1999], *Slemr et al.* [1998, 2001]
P	3 July 1995, 24 September 1997, 23 October 1997	B747, DC10, B747, A340-300, DC8	240, 265, 260, 480, 690	wide-body aircraft plume particles and gaseous emissions, intercomparison between Falcon, A340 and DC8, gaseous sulfuric acid from the DC8; Falcon	*Schulte et al.* [1997], *Konopka et al.* [1997], *Tremmel et al.* [1998], *Helten et al.* [1999], *Schumann et al.* [2000a]
6	28–30 September 1998	ATTAS; B737-300	2.6 ± 0.3/118 ± 12; 2.6 ± 0.3/56 ± 6; 2.6 and 66 at ground	first detailed resolution of nuclei mode size range by 8–9 particle counters with 3–60 nm cutoff sizes, for two aircraft, and sulfuric acid and ion concentrations; Falcon and ground behind ATTAS	*Petzold et al.* [1999], *Schröder et al.* [2000b], *Arnold et al.* [2000], *Curtius et al.* [2002], *Brock et al.* [2000], *Wohlfrom et al.* [2000]
7	15 September 1999	A340-300; B707-307C	120 ± 12; 380 ± 25	test of impact of engine efficiency and measurements of aerosol and large ion clusters in young plumes (0.25–1 s); Falcon	*Schumann* [2000], *Schumann et al.* [2000b], this work

[a]Numbers including "P" for POLINAT.

investigate particle formation from various aircraft, burning fuels with different FSCs during the same flight. The experiments S1–S7 included 10 flights with measurements in the young exhaust plume of various aircraft at separation distances varying from 25 m to about 5 km (plume ages 0.15–30 s, see Figure 1a, for example), and measurements at ground during S3 to S6. The measurements inside and outside of aircraft plumes have been performed on board the Falcon aircraft of DLR, see Figure 1b. Ground experiments were performed to measure particles and particle precursors close to jet engine exit.

[9] The observations have been performed with an increasingly refined set of instruments by various partners, see Table 2, as described in detail in the individual papers listed. The instruments include innovative methods, such as four different mass-spectrometer instruments of MPIK, and a system of instruments to measure the number, size and volatility of aerosols in the diameter range from 3 nm to 20 μm of DLR-IPA and partners.

[10] In most of the experiments the DLR Advanced Technology Testing Aircraft System (ATTAS) was used as the aircraft causing the exhaust, see Table 3. The ATTAS is a midsized two-engine jet aircraft of type VFW 614, with Rolls-Royce SNECMA M45H Mk501 engines, see Figure 1c, built in 1971 [*Busen and Schumann*, 1995]. In more

recent experiments, also younger and larger jet aircraft were investigated; their engines have higher thrust, bypass ratio, and pressure ratio. Higher bypass engines offer higher overall propulsion efficiency causing less waste heat released into the plume gases [*Cumpsty*, 1997], which impacts contrail formation [*Schumann*, 1996a, 2000]. The fuel sulfur conversion fraction depends probably on combustion pressure [*Brown et al.*, 1996b], which increases with the pressure ratio.

[11] The experiments cover a wide range of FSC values. Aviation fuels are produced with FSC values from near 1 μg/g to an upper limit of 3000 μg/g. The median FSC value of fuels provided for airliners is near 400 μg/g [*IPCC*, 1999]. In cases S1, S6, and S7 the FSC was varied by using different fuel deliveries. In cases S2–S5, up to 60 kg of dibuthylsulfide ($C_8H_{18}S$) containing a 22% mass fraction of sulfur were added to one of the fuel tanks to increase the FSC relative to the fuel in other tanks to the desired level. The melting-, boiling-, and flame-point temperatures and the density of the additive ($-80°C$, $182°C$, $62°C$, 840 kg m^{-3}) are sufficiently similar to those of standard Jet-A1 kerosene fuel ($-50°C$, 164 to $255°C$, $52°C$, 800 kg m^{-3}) to allow for reasonable mixing, and the additive can be handled easily. Later, other experimenters used tetrahydro-thiophene (C_4H_8S; $-96°C$, $120°C$, $12°C$, 1000 kg m^{-3}) for
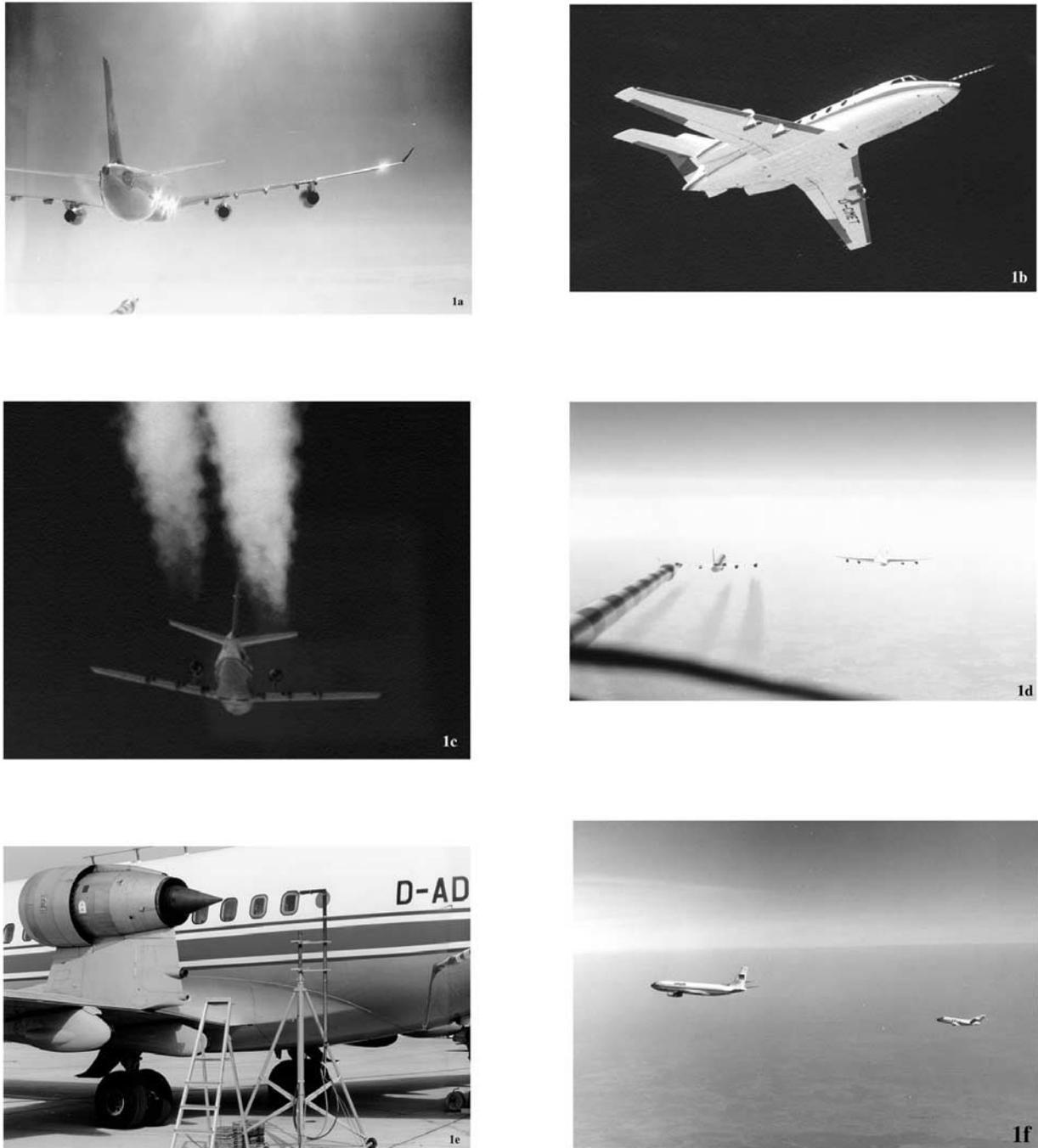
Figure 1. (a) Photo of the Airbus A340 at cruise during S7 measuring about 70 m behind the right turbofans. The nose boom of the Falcon used for turbulence measurements is visible at the lower edge of the photo; (b) the Falcon with particle measurement systems below the wing and aerosol inlet at top of the fuselage during S4; (c) the ATTAS at cruise during S2 burning low (high) fuel sulfur content on left (right) engine; (d) the A340 and the B707, wing by wing, one with, the other without contrails during S7; (e) sample inlet behind the ATTAS engines at ground during S3; (f) Falcon measuring in the B707 plume 70 m behind the engines during S7. See color version of this figure at back of this issue.

this purpose [*Cofer et al.*, 1998; *Miake-Lye et al.*, 1998] which shows larger differences to kerosene. The FSC was analyzed from fuel samples with standard laboratory methods or inferred from the amount of sulfur added to a reference fuel. The reproducibility of sulfur analysis from the same sample in various laboratories with 95% confidence interval is better than 10% [*Schröder et al.*, 2000b]. Larger differences (maximum of 25%, S5) were found

Table 2. Instruments Used in the Various Experiments

Instrument	Measured Parameter	Method	S1	S2	S3	S4	S5	P	S6	S7	Operator[a]	Reference
Video, photos, cockpit instruments on Falcon	contrail onset, flight level, speed	standard instruments of the Falcon (S1: Piper Cheyenne IIIA)	X	X	X	X	X	X	X	X	DLR	Schumann et al. [1996]
PT100 and PT500	temperature	standard instrumentation of the Falcon		X	X	X	X	X	X	X	DLR	Schumann et al. [1996]
Five-hole pressure transducer, horizontal position	pressure, turbulent wind components, position	standard instrumentation of the Falcon		X	X	X	X	X	X	X	DLR	Bögel and Baumann [1991]
Vaisala HMP35	H_2O, relative humidity	capacitive polymer humicap-H		X		X	X	X	X	X	DLR	Ström et al. [1994]
Lyman-alpha hygrometer	H_2O, mixing ratio	Buck research hygrometer		X							DLR	Ström et al. [1994]
Frost point	H_2O, frost point	frost point mirror, Buck				X	X		X	X	DLR	Busen and Buck [1995]
CPC	condensation nuclei (CN), particle concentration with $d > 7$ nm, $d > 18$ nm	modified TSI 3760, condensation particle counters (CPCs), interstitial aerosol inlet		X		X					University of Stockholm	Schumann et al. [1996]
CPC	$d > 5, 10, 14$ nm volatile and nonvolatile aerosols ($d > 14$ nm for S5, $d > 10$ nm for S6 and S7)	modified TSI 3760A and 3010 CPCs with interstitial aerosol inlet, operated with heated sample (in S5 alternatively)				X	X	X	X	X	DLR	Petzold et al. [1997]
CPC	$d > 3$ nm	ultrafine CPC, modified TSI 3025, interstitial aerosol inlet				X			X	X	DLR	Schröder et al. [1998]
N-MASS	number concentration for particles with $d > 4, 8, 13, 30, 55$ μm	CN counter cascade							X		University of Denver	Brock et al. [2000]
PCASP	dry aerosol size distribution, $0.1 < d < 1$ μm, 32 channel resolution (20 used)	PMS passive cavity aerosol spectrometer probe, PCASP-100, internal, interstitial aerosol inlet		X							University of Stockholm	Schröder and Ström [1997]
PCASP	dry aerosol size distribution, $0.1 < d < 3$ μm, 15 channel resolution	PMS PCASP-100, wing station				X	X	X	X	X	DLR	Schröder and Ström [1997]
FSSP 100	cloud element size distribution, 1 μm $< d <$ 16 μm	forward scattering spectrometer probe (FSSP), Particle Measurement Systems (PMS)		X							DLR	Schröder and Ström [1997]
FSSP-300	aerosol and cloud size distribution, 0.35 μm $< d <$ 20 μm	FSSP, PMS				X	X	X	X	X	DLR, S4: University of Mainz	Schröder et al. [2000a, 2000b], Borrmann et al. [2000]
PSAP	integral soot mass, absorption coefficient	soot photometer, filter deposition technique					X		X		DLR	Petzold et al. [1999]
MASP	aerosols sizes and forward/backward scattering ratio, 0.4 μm $< d <$ 10 μm	multiangle scattering spectrometer probe				X					DLR and NCAR	Kuhn et al. [1998]
MASS	size distribution, ~12 nm $< d <$ 0.4 μm	Mobile Aerosol Sampling System			(X)	X		X			UMR	Hagen et al. [1996]
Integrating Nephelometer	scattering coefficient	integrating volume scattering technique					X		X	X	DLR	Petzold et al. [1999]

Table 2. (continued)

Instrument	Measured Parameter	Method	S1	S2	S3	S4	S5	P	S6	S7	Operator[a]	Reference
CIMS	trace gases SO_2, HONO, HNO_3	Chemi Ionization Mass Spectrometry						X				Arnold et al. [1992, 1994]
SIOMAS	small chemiions (1–220 in S3; 1–450 amu in S4 and S5)	Small Ion-Mass Spectrometer			X	X	X				MPIK	Arnold et al. [1998a, 1998b]
LIOMAS	large positive and negative chemiions (1–8500 amu)	Large Ion-Mass Spectrometer						X	X	(X)	MPIK	Wohlfrom et al. [2000]
VACA	total (gaseous and evaporated liquid) H_2SO_4	Volatile Aerosols Component Analyzer: CIMS with NO_3^- ions and heated inlet			X		X	X	X		MPIK	Curtius et al. [1998], Curtius and Arnold [2001]
Gerdien condenser	positive total ion concentration	electrostatic probe								X	MPIK	Arnold et al. [2000]
NDIR CO_2 sensor	carbon dioxide (CO_2) concentration	nondispersive infrared differential absorption					(X)	X	X		DLR	Schulte et al. [1997]
GPS	distance	Differential Global Positioning System					X	(X)	(X)		DLR	
Grab samples	NMHC concentration	grab samples analyzed for hydrocarbons and CO by gas chromatography					X				FhG/IFU	Slemr et al. [2001]
VUV fluorescence CO	carbon monoxide (CO) concentration	vacuum ultraviolet fluorescence								X	DLR	Gerbig et al. [1996]
Emission measurement system	EI of CO_2, CO, HC, NO_x, NO, soot smoke number (SN)	ICAO standardized instruments			X						MTU	ICAO [1981]

[a]DLR, Deutsches Zentrum für Luft- und Raumfahrt, Oberpfaffenhofen; FhG/IFU: Fraunhofer-Institut für Atmosphärische Umweltforschung, Garmisch-Partenkirchen; MPIK: Max-Planck-Institut für Kernphysik, Atmospheric Physics Division, Heidelberg; MTU: Motoren und Triebwerk Union, München; NCAR: National Center for Atmospheric Research, Boulder, Colorado; UMR: University of Missouri-Rolla, Rolla, Missouri Entries with parentheses (X) denote instrument applications with reduced data output.

Table 3. Aircraft and Engines Investigated

Aircraft	Engine	Year[a]	Bypass Ratio	Pressure Ratio	Thrust, kN	Experiment
B707-307C	PW JT3D-3B	1968	1.4	13.6	80.1	S7
ATTAS	Mk501	1971	3.0	16.5	32.4	S1–S6
B747-200B	JT9D-7J	1971, 1976	5.1	23.5	222.4	POLINAT
DC10-30	CF6-50C	1974	4.3	27.8	224.2	POLINAT
B737-300	CFM56-3B1	1987	5.1	22.4	89.4	S6
A310-300	CF6-80C2A2	1991	5.1	28	233.3	S4
A340-300	CFM56-5C2	1993	6.8	28.8	138.8	POLINAT
DC8	CFM56-2C1	1994	6.0	~23.5	~97.9	POLINAT
A340-300	CFM56-5C4	1998	6.6	31.1	151.2	S7

[a]The year is the year of engine construction; the bypass ratio is the ratio of the mass flux through the outer fan duct of the engine relative to the mass flux through the core duct of the engine at takeoff; the pressure ratio is the ratio between pressure at combustor inlet and at engine inlet at takeoff; the thrust is given for takeoff [ICAO, 1995].

between FSC analysis of fuel samples and FSC values derived from the amount of sulfur added, possibly due to incomplete mixing and partial evaporation of the additive. For the two B747 aircraft and the DC10 during POLINAT the FSC is determined from SO_2 and CO_2 measurements in the plume with about 30% accuracy [Arnold et al., 1994; Schulte et al., 1997; Schumann et al., 2000a].

[12] Table 4 lists the parameters during the flight measurements reported. The aircraft were operated mainly in the upper troposphere, with or without contrails or at threshold

Table 4. Atmospheric Conditions During the In-Flight Measurements

Experiment[a]	Aircraft, Case	Date	FL, hft	FSC,[b] µg g^{-1}	p, hPa	T, °C	RH, %	V, m s^{-1}	η	T_c,[c] °C	Contrail Seen
S1	ATTAS	13.12.94	299	2, 250	302.3	−49.7	44	115	0.14	−49.6	threshold
S2	ATTAS, C1	22.3.95	288	170, 5500	317	−49.0	42	163	0.172	−48.8	threshold
	C2		290	170, 5500	316	−49.5	36	163	0.175	−49.1	threshold
	C3		290	170, 5500	315	−49.2	37	163	0.182	−49.3	threshold
	C4		290	170, 5500	316	−48.3	37	163	0.198	−48.8	threshold
	low/high		310	170, 5500	287	−55	40	163	0.168	−50	yes
	high/high		300	5500	301	−51.3	45	163	0.171	−50	yes
S4	ATTAS	12.3.96	240	6, 2830	392.7	−39	10	160	0.17	−48.3	no
			310	6, 2830	287.4	−43	20	175	0.17	−50.9	no
	A310	13.3.96	350	850, 2700	238.4	−58	15	180	0.28	−51.6	yes
	ATTAS	15.3.96	310	6, 2830	287.4	−52.3	40	165	0.17	−50.1	yes
			270	6, 2830	344.3	−42	45	160	0.17	−48.1	no
S5	ATTAS	16.4.97	250	22	376	−44	30	160	0.17	−48.0	no
	H$_2$SO$_4$ inject.		310	22	287	−52	45	160	0.17	−49.9	yes
	ATTAS	18.4.97	260	24, 2700	360	−42	50–65	160	0.17	−46.4	no
			310	24, 2700	287	−54	90–65	165	0.17	−48.7	yes
P	B747-200B	3.7.95	330	240	262	−46	17	257	0.33	−49.7	no
	DC10-30	3.7.95	330	265	262	−45	18	255	0.33	−49.7	no
	B747-200B	3.7.95	330	260	262	−45	21	255	0.33	−49.6	no
	A340-300	24.9.97	350	480	238.4	−51	29	200	0.3	−50.1	yes
	DC8	23.10.97	330	690	261	−49	57	227	0.3	−47.8	yes
S6	ATTAS	28.9.98	260	2.6, 118	359	−38	35–40	153	0.17	−47.9	no
			320	2.6, 118	274	−52	35–50	177	0.17	−50.8	yes
	B737	30.9.98	190	2.6, 56	490	−14	75–85	141	0.3	−39.5	no
			260	2.6, 56	360	−30	55–65	167	0.3	−44.7	no
			350	2.6, 56	238	−52	>60	192	0.3	−49.2	yes
			370	2.6, 56	216	−56	>65	199	0.3	−49.8	yes
S7	B707	15.9.99	310	120	288	−42	20	187	0.25	−50.0	no
			334	120	256.05	−49.3	38	190	0.31	−49.4	threshold
	A340		336.6	380	252.34	... 50.42	42	195	0.23	−50.6	threshold
			349	380	245.32	−50.9	34	209	0.24	−51.0	threshold
	B707		342	120	247.65	... 50.54	33	203	0.28	−50.4	threshold
	A340		314	380	281	−42	20	194	0.27	−50.0	no

[a]Experiment name, date, flight level (FL, 1 hft = 100 feet = 30.48 m), fuel sulfur content (FSC), ambient pressure (p), temperature (T), relative humidity of liquid saturation (RH), true air speed V, overall propulsion efficiency η, computed contrail threshold temperature (T_c), and report on whether a contrail was seen or not.

[b]The fuel analyses (~20 samples) imply a combustion heat $Q = 43.21 \pm 0.06$ MJ kg^{-1}, and a hydrogen mass fraction of 13.71 ± 0.1% ($EI_{H2O} = 1.225 \pm 0.01$; $EI_{CO2} = 3.16 \pm 0.005$).

[c]T_c is computed for the measured fuel properties and the estimated overall propulsion efficiency η using the Schmidt/Appleman criterion with code available from http://www.op.dlr.de/ipa/schumann/.

conditions where contrails were just forming or disappearing. Some of the chased fast aircraft were operated at reduced power settings to let the slower Falcon follow at close distance.

3. Results

3.1. Visual Observation of Contrail Formation Independent of FSC During SULFUR 1

[13] As a test for postulated influences of sulfur emissions on nucleation, the contrail formation from the ATTAS was investigated using fuels with different FSCs (2 and 250 μg/g) on the two engines during the same flight [*Busen and Schumann*, 1995]. Contrail formation was observed visually from another aircraft following at close distance and documented in photos and videos. Ambient temperature and humidity were deduced from a nearby radiosonde at flight level. At threshold conditions, short contrails were seen to form about 30 m behind the engines. Other than expected from previous discussions on the importance of fuel sulfur for particle formation, the observations, photos and videos revealed no systematic difference in the contrails forming from the two engines.

[14] However, the contrail did form at a temperature that was about 2 K warmer than expected from the Appleman criterion. This difference is not caused by sulfur emissions but by effects of the overall propulsion efficiency η not included in the Appleman criterion [*Busen and Schumann*, 1995]. The higher the value of η, the less combustion heat leaves the engine exit with the exhaust, allowing contrails to form at higher ambient temperature [*Schmidt*, 1941]. The value of $\eta = VF/(Q\,m_f)$ depends on the aircraft speed V, thrust F, specific fuel combustion heat Q, and fuel consumption rate m_f [*Schumann*, 1996a]. With $(1-\eta)\,Q$ as effective combustion heat, the Schmidt/Appleman criterion fits the observed threshold temperatures for contrail formation to better than 0.5 K (see Table 4).

[15] The threshold temperature is computed assuming that heat and water vapor in the exhaust are well mixed when leaving the engine and that the plume reaches liquid saturation locally during mixing. However, water is emitted only from the core engine while heat is emitted from both the core and the bypass of the engine, implying nonuniform exit conditions. Moreover, part of the combustion heat leaves the engine with the jet as kinetic energy and is dissipated to heat during mixing of the jet with ambient air [*Schumann*, 1996a]. Therefore the humidity in the plume deviates slightly from what is expected according to the Schmidt/Appleman concept. A model computation for the S1 conditions revealed a local liquid water supersaturation of about 7%, enough to let fresh soot particles larger than 30 nm diameter become activated and form water droplets even at threshold conditions [*Schumann et al.*, 1997]. If soot would be hydrated before reaching liquid saturation, contrails could form at slightly higher ambient temperature [*Kärcher et al.*, 1996b]; a 10% lower critical humidity increases the threshold temperature, which is typically below −40°C, by 0.9 to 1.1 K. The liquid droplets formed freeze quickly and then grow further by water deposition because of high ice supersaturation. Homogeneously nucleated sulfuric acid droplets do not freeze and grow fast enough under threshold conditions to form a visible contrail [*Kärcher et al.*, 1995]. The number of ice particles formed must be larger than $10^4\,cm^{-3}$

in order to produce a visible contrail as early as observed [*Kärcher et al.*, 1996b]. The water droplets freeze at timescales of the order of milliseconds and the accommodation coefficient of water vapor molecules on the ice surface is at least 0.2 to allow for particle growth as fast as observed in this experiment [*Schumann*, 1996b].

3.2. Discovery of Fuel Sulfur Influence on Particle Formation During SULFUR 2

[16] The S2 experiment was performed to cover larger FSC values and to measure the properties of particles formed as a function of FSC [*Schumann et al.*, 1996]. Again, the ATTAS aircraft was used as exhaust forming aircraft. Different FSC values of 170 and 5500 μg/g were prepared by using a standard fuel with 170 μg/g in one aircraft fuel tank and by adding dibuthylsulfide to the fuel in the other tank. Besides photo and video observations from close distance, in situ measurements were made flying the Falcon aircraft in the wake of the ATTAS at plume ages of about 20 s, at altitudes between 9 and 9.5 km, and temperatures between −49° and −55°C, when the visible contrail extended to about 2 km length.

[17] Besides standard instruments available on the Falcon, the instruments (see Table 2) included two CPCs with cutoff sizes of 7 and 18 nm, and a Passive Cavity Aerosol Spectrometer Probe (PCASP) counting optically the dried aerosol larger 120 nm in diameter after entering the measurement systems inside the aircraft via an "interstitial," i.e., backward facing sample inlet at top of the fuselage outside the boundary layer, and a Forward Scattering Spectrometer Probe (FSSP-100) of Particle Measurement Systems Inc. (PMS) mounted outside the aircraft at a wing station for particles larger than 1 μm.

[18] The observations demonstrated that fuel sulfur emissions do cause measurable and even visible changes in the particle properties and contrails. At ambient temperatures 5 K cooler than the threshold temperature for contrail onset, the plume was visible already about 10 m behind the engine exit for high FSC, but 15 m behind the engine exit for low FSC (see Figure 1c). During descent through the level of contrail onset the high sulfur contrail remained visible at slightly lower altitude (25 to 50 m) or higher temperature (0.2 to 0.4 K). The higher FSC caused a larger optical thickness of the contrail shortly after onset. The high FSC contrail grew more quickly but also evaporated earlier than the low FSC contrail. At plume ages of about 20 s each engine plume was spread to about 20 m diameter. The plumes contained many subvisible particles. Peak number densities were 30,000 cm^{-3} for particles of diameter above 7 nm and 15,000 cm^{-3} above 18 nm. The particle measurements at low FSC indicate that the number of particles larger than 7 nm measured in the plume originated mainly from emitted soot particles. The number of particles in this size range increases by about 25% for particle of diameter above 7 nm and by 50% for particles above 18 nm when the FSC is increased by a factor of 30. The results suggest that part of the fuel sulfur is converted to sulfuric acid which interacts with the soot. Hence sulfuric acid tends to "activate" soot particles [*Kärcher et al.*, 1996b]. Estimates of the number, size, and volume of the particles reveal that the measurements are consistent with estimated soot emission indices (EIs) and some volatile material from sulfur to

Table 5. Emission Parameters of the ATTAS Engines at Ground and at Cruise

Parameter[a]	Unit	Origin	Ground,[b] power, %						Cruise (Origin)
			7	18.5	30	57.5	85	100	
EI_{NOx}	g(NO$_2$) kg^{-1}	MTU	1.9	3.0	4.1	6.7			5–9[c]
		ICAO	1.5		3.6		9.3	11.5	
EI_{NO}	g(NO$_2$) kg^{-1}	MTU	1.0	1.2	2.1	4.0			0.8–1.5[c]
		IFU	<1.9	<1.7	<2.1		3.9		
		DLR		0.1	1		3.4		
EI_{CO}	g kg^{-1}	MTU	112.	52.	24.	6.			12–22[d]
		ICAO	178.		51.		7.9	6.2	
		IFU	125	59	26		5.6		
		DLR	104	50	22		4.8		
EI_{HC}	g kg^{-1}	MTU	31.	6.	2.	0.4			0.02–0.25[d]
		ICAO	59.5		7.4		0.74	0.75	
EI_{soot}	g kg^{-1}	DLR	0.013	0.045	0.13		0.4		0.1–0.15[e]
SN		MTU	2	5	10	24			
		ICAO	2.7		10.9		38.4	46.3	
m_f	kg s^{-1}	MTU	0.054	0.099	0.146	0.270			0.12[f]
		ICAO	0.053		0.146		0.416	0.498	0.22[d]
T_C	K	RR	678		683		746	760	617[f]
T_B	K	RR	293		293		292	295	237.5[f]
T	K	IFU	561	585	615		647		620–655[c]
		DLR	586	605	635		668		
V_C	m s^{-1}	RR	80		172		357	414	417[f]
V_B	m s^{-1}	RR	96		180		274	290	248.2[f]

[a]Emission indices (EIs) for nitrogen oxides (NO$_x$) and nitric oxide (NO, in mass units of NO$_2$) for carbon monoxide (CO) and for nonmethane hydrocarbons (HC, in mass units of CH$_4$); smoke number (SN); fuel flow rate (m_f); core exit static temperature (T_C); bypass exit static temperature (T_B); gas static temperature (T) measured 1.8 m past engine nozzle exit; core exit jet speed (V_C), bypass exit speed (V_B), for various power settings in percent of full power at ground and for observed cruise conditions.

[b]Ground measurements during SULFUR 3 and 4 behind the ATTAS by Motoren and Triebwerk Union (MTU, G. Huster, personal communication, 1995) from measurements reported in the ICAO emission database [*ICAO*, 1995] and from FTIR emission spectrometry by Fraunhofer-Institut für Atmosphärische Umweltforschung (IFU) [*Heland and Schäfer*, 1998; J. Heland, personal communication, 1996] and by *Haschberger et al.* [1997] (DLR); and as derived from engine performance data provided by Rolls-Royce (RR). The MTU values are mean values over three measurements: One from the right wing engine with low FSC (218 µg/g), one from the left wing engine with low FSC (218 µg/g), and one from the left wing engine with high FSC (2800 µg/g), without significant differences and with relative deviations of a few percent.

[c]*Haschberger and Lindermeir* [1997].

[d]Range of data for various plume encounters from *Slemr et al.* [2001].

[e]*Petzold and Döpelheuer* [1998].

[f]Engine computations for conditions of S1; for S2, see *Schumann et al.* [1996].

sulfuric acid conversion at a fraction ε of about 0.4% or little larger, as suggested by *Frenzel and Arnold* [1994]. Color differences were observed between contrails formed from two engines burning fuels with different FSC and this color difference can be explained with more but smaller ice particles for higher FSC [*Gierens and Schumann*, 1996].

[19] The results of S1 and S2 were used to guide and test model studies in many follow-up papers [*Kärcher*, 1996, 1998a, 1998b; *Kärcher et al.*, 1996b, 1998a; *Brown et al.*, 1996b, 1997; *Gleitsmann and Zellner*, 1998a, 1998b, 1999; *Konopka and Vogelsberger*, 1997; *Andronache and Chameides*, 1997, 1998; *Taleb et al.*, 1997; *Lukachko et al.*, 1998; *Yu and Turco*, 1997, 1998a; *Jensen et al.*, 1998a, 1998b; *Garnier and Laverdant*, 1999; *Tremmel and Schumann*, 1999; *Zaichik et al.*, 2000; *Starik et al.*, 2002]. In particular, *Yu and Turco* [1998a] showed that the measurements can be quantitatively reproduced to good approximation with a plume aerosol model assuming ε = 1.8%, when including enhanced coagulation by CIs in the model. The relatively strong increase of the observed number of particles >18 nm compared to that >7 nm is caused by scavenging of vapors and particles by ice particles in the young contrail which then leave the aerosol measured after evaporation. The remaining sulfate aerosol accumulation mode may contribute to cloud condensation and ice nuclei. The observations and the model studies show that the FSC does not influence the threshold temperature for contrail formation but does influence the optical appearance of the contrail. An increase in FSC is likely to cause more sulfuric acid in the plume and by a combination of homogeneous and soot-induced heterogeneous freezing more particles which grow by water uptake, freeze, and form ice particles [*Kärcher et al.*, 1998a].

3.3. Ground-Based Gaseous and Ion Emission Measurements During SULFUR 3

[20] A ground-based experiment was performed to insure that the differences measured between the left and right engine exhaust plumes originate from different FSC and are not caused by engine differences. Moreover, this experiment was used for emission measurements very close to the engine exit, including the first mass spectrometric measurements of negative and positive CIs, and of gaseous H$_2$SO$_4$ and SO$_3$ in the exhaust at plume ages of 6 to 20 ms [*Arnold et al.*, 1998a]. Similar measurements were also performed behind a JT9D-7 engine in the jet-engine testing facility of Lufthansa at Hamburg at 18.6 m distance, 170 ms plume age [*Arnold et al.*, 2000].

[21] The EIs of NO, NO$_x$, CO, HC, and the smoke number of the ATTAS engines were measured at ground using instruments satisfying International Civil Aviation Organization (ICAO) standards [*ICAO*, 1981]. The samples were taken behind the ATTAS at the same position (centerline, 1 m behind engine exit cone, 1.8 m behind engine nozzle exit, see Figure 1e) for various power settings and

FSC values, see Table 5. The measured values show the same trends with power as the ICAO data but with 20% higher EIs for NO_x and about 50% lower values for CO and HC compared to the values reported by *ICAO* [1995]. The lower EI_{CO} values are also supported by simultaneous Fourier transform infrared spectrometer (FTIR) measurements performed during S4 at ground and in flight [*Haschberger et al.*, 1997; *Heland and Schäfer*, 1998]. *ICAO* [1995] contains no information on the NO/NO_x ratio. The measurements indicate that about 30 to 50% of the NO_x is emitted as NO_2; smaller values have been derived during cruise from FTIR measurements (NO_2/NO_x ratio of 12–22%) [*Haschberger and Lindermeir*, 1997]. Anyway, the NO_2/NO_x fraction measured for the ATTAS is far higher than for the RB211-524 engine [*Schumann*, 1995], which emits less than 5% of all NO_x as NO_2, possibly due to higher combustion temperature and pressure. The emission data obtained behind the left and right wing engine of the ATTAS, and for different FSC values (with different amounts of additives), show no significant differences. Hence any difference measured in the plumes is not caused by engine differences. Moreover, the FSC has no detectable influence on the emission index values listed, including the smoke number. The basic emissions including soot seem to be invariant to FSC. These measurements have been used for comparison to in-flight measurements of EIs of CO and HC by *Slemr et al.* [1998, 2001]. As a result, the ATTAS engine is one of the best characterized engines described in the open literature, well suited for modeling.

[22] Mass spectra of negative and positive CIs were measured using a quadrupole Ion Mass Spectrometer (IOMAS). Gaseous H_2SO_4 and SO_3 were measured using a Chemical Ionization Mass Spectrometer (CIMS). For these measurements the exhaust is passed through a flow tube system containing a capillary ion source. The source introduces nitrate-ions (mostly $NO_3^-(HNO_2)_n$, $n = 0, 1, 2$) into the flow tube which react with gaseous H_2SO_4 and SO_3 present in the exhaust to form HSO_4^- ions and $NO_3^-SO_3^-$ ions, respectively. Analyzing the ion composition in the flow tube downstream of the source, the number density of H_2SO_4 and SO_3 can be determined for given reaction time and rate coefficients of the respective ion-molecule reactions. The results show a total negative ion concentration of more than 1.4×10^7 cm^{-3} at plume ages of around 10 ms in the exhaust of a jet engine at the ground [*Arnold et al.*, 1998a]. For low FSC the S^{VI} concentration was measured implying a conversion fraction ε of 1.2%. For high FSC most of the sulfuric acid formed ions HSO_4^- $(H_2SO_4)_m$ with $m > 1$ with masses outside the range detectable by the IOMAS instrument (220 atomic mass units, amu). This finding initiated new experiments using mass spectrometers with larger mass ranges as described below.

3.4. Comparison of Exhaust From Different Aircraft During SULFUR 4

[23] In order to generalize the results to other aircraft, with more modern engines, and to search for sulfuric acid in the exhaust plume of cruising aircraft, an experiment was organized in which the Falcon could measure in the young exhaust plume of an Airbus A310 at cruise (plume ages 1–4 s), and behind the ATTAS with refined instruments, at very close approach (plume age 0.5–1 s), for situations with and

without contrail formation and for a large range of FSC values (6 to 2830 μg/g) [*Petzold et al.*, 1997]. The close approach of the Falcon to the ATTAS and Airbus aircraft was made possible by the Falcon pilots after learning about the nature of wake vortex formation [*Gerz and Holzäpfel*, 1999]. Steady flight conditions could be reached at some positions within the wake vortex as close as 25 m (during S6) behind the leading aircraft by expert pilots. Steady flight is not possible at plume ages of about 5 to 20 s when the wake vortices are fully developed and break up into small-scale turbulence [*Gerz et al.*, 1998; *Holzäpfel et al.*, 2001].

[24] During S4, new PMS-type optical spectrometers were implemented: A PCASP-100 (0.1–3 μm dry diameter) and a FSSP-300 (0.35–20 μm), both mounted outside the Falcon fuselage. For the first time the spectral distribution and variability of larger aerosol and contrail ice crystals in young exhaust plumes have been documented. The ice crystal mean mode was located around 1 μm. The particle size distributions exhibit strong variations from the plume center to the diluted plume edge. The number of ice particles in the contrails were found to increase by about a factor 1.3 to 2.7 with contrail age. At 10 s plume age the number of detected particles with size >10 nm increases by a factor of 1.3 for an increase of FSC by a factor of 500.

[25] No systematic difference was found at lower plume ages (<3.3 s) in the A310 for different FSC values. However, the FSSP-300 was originally designed for low to moderate aerosol particle concentrations with corrections becoming necessary above typically 500 cm^{-3}. Hence the number of ice particles was underestimated in S4 by more than a factor of 2 [*Schröder et al.*, 2000a], leaving the possibility for a stronger sensitivity of crystal concentrations to FSC.

[26] The soot (black carbon) EI of the ATTAS engines was determined from soot size spectra measured at ground and during flight. Converted to cruise conditions with about 50% of full power, the soot mass EI amounts to 0.15 g kg^{-1} [*Petzold and Döpelheuer*, 1998]. Before these measurements, a larger EI was expected (about 0.5 g kg^{-1} [*Schumann et al.*, 1996]). Measurements of the refractive index of ice particles were found to be consistent with a large fraction of soot entering the ice particles [*Kuhn et al.*, 1998]. This was confirmed by ice crystal residuum analysis [*Petzold et al.*, 1998]. Soot collected on filters sampled at ground closely behind the engines contained sulfate. Ion chromatography measurements indicated 0.5% conversion of fuel sulfur to sulfate in the soot, with only a slight dependence on engine power setting. Organic carbon was found to contribute up to 40% to the carbonaceous fraction of soot particles at typical cruise conditions [*Petzold and Schröder*, 1998].

[27] Negative ions observed with the Small Ion-Mass Spectrometer (SIOMAS, an improved version of IOMAS) inside the plume of an Airbus A310 aircraft in flight at altitudes around 10.4 km at plume ages of about 2–3 s were mainly HSO_4^- $(H_2SO_4)_m$, HSO_4^- $(HNO_3)_m$, and NO_3^- $(HNO_3)_m$ ions with $m \leq 2$ [*Arnold et al.*, 1998b]. No negative CIs from the engine were found. It seems that the negative CIs grow rapidly, reaching mass numbers greater than measured (1100 amu) at a plume age of 3 s. The upper limit for the mean positive CI concentration estimated on the base of the measurements was about $3 \times$

10^5–3×10^6 cm^{-3}. This number is very close to the maximum possible ion concentration allowed by ion-ion recombination processes in the young exhaust plume. Dilution alone [*Schumann et al.*, 1998] implies about 300 times larger concentrations at engine exit.

[28] These measurements did not detect gaseous H$_2$SO$_4$ [*Arnold et al.*, 1998b; *Petzold et al.*, 1997]. Only an upper limit for the gaseous H$_2$SO$_4$ concentration of $<2 \times 10^8$ cm^{-3} could be obtained with SIOMAS. Any H$_2$SO$_4$ vapor initially formed experiences rapid gas-to-particle conversion at plume ages <1.6 s, as expected from model results [*Kärcher et al.*, 1995].

3.5. Ultrafine Aerosols, Ions, and Sulfuric Acid Detected During SULFUR 5

[29] Shortly after S4, NASA colleagues performed similar experiments during a series of measurements in the SUCCESS project in April–May 1996 [*Toon and Miake-Lye*, 1998]. Moreover, first results were reported from the SNIF missions performed behind various jet aircraft (MD80, B727, B737, B747, B757, DC8, T-38) in January–May 1996 [*Anderson et al.*, 1998a, 1998b; *Cofer et al.*, 1998]. A strong increase of the number of volatile particles with FSC was found in the young plume [*Miake-Lye et al.*, 1998]. In the first preliminary presentation of the results of these measurements during a Conference at Virginia Beach in April 1996 it was suggested that the conversion fraction could reach up to 70%. Later publications on these experiments concluded ε values of 8 to 15% [*Anderson et al.*, 1998b], 31% (based on CIMS measurements of SO$_2$, analyzed FSC of the fuel used, and in situ CO$_2$ measurements) [*Miake-Lye et al.*, 1998], 26% [*Hagen et al.*, 1998], and 37% [*Pueschel et al.*, 1998]. The CIMS measurements during SUCCESS behind a B757 indicated that the conversion fraction increases from 6% for low FSC (72 µg/g) to 31% for high FSC (676 µg/g). In discussing the differences, it was argued that the S2 measurements might possibly underestimate the fraction of ultrafine particles [*Anderson et al.*, 1998b]. Therefore we performed a further experiment with enhanced capability to measure volatile and also nonvolatile fractions of ultrafine particles, and sulfuric acid in the gas phase and in the liquid particle phase, see below.

[30] Compared to S4, the fine mode aerosol sampling system (CPCs with $d > 5$ and 14 nm) was principally modified by a passive sample dilution to increase the detectable particle concentration range to about 5×10^5 cm^{-3} [*Schröder*, 2000]. A heating section was introduced to (alternatively) evaporate the volatile aerosol fraction for exclusive detection of the soot particle number density. Further, an infrared CO$_2$ sensor, a frost point hygrometer, two different mass spectrometer instruments, and canisters for air grab sampling were added to the Falcon payload, see Table 2.

[31] The Falcon chased the ATTAS at two altitudes and at distances between 70 and 3100 m. Fuels with low and high FSC (22 ± 2 and 2700 ± 350 µg/g) were used at conditions with and without contrail formation, see Table 4.

[32] Aerosol measurements were presented by *Schröder et al.* [1998]. Soot emissions were found to show no significant dependence on FSC. Evidence was given that at least 1/3 of the soot particles was lost from the interstitial aerosol. Thus soot has been involved in the ice nucleation

process, possibly in addition to freezing of newly formed volatile particles. For the ultrafine ($d = 5 - 14$ nm) volatile aerosol a distinct increase of the apparent EIs within the first 10 s plume age was documented for the first time, illustrating the dynamic growth processes of freshly produced aerosol past exit. Further, the S5 measurements revealed differences between volatile particle formation within and outside contrail environment. In the absence of contrails the number of volatile particles with diameters >5 nm reaches 10^{17} kg^{-1} for high FSC and still reaches 10^{16} kg^{-1} for low FSC. In contrails, ultrafine particles were found diminished by significant fractions, most likely due to scavenging by ice crystals in the aging plume. A clear correlation between FSC and volatile particle growth was observed. The size spectra are bimodal with many volatile particles for large FSC in a diameter range near 14 nm.

[33] The observations provided important data to test models of aerosol formation in engine plumes. Model studies showed that the observed growth of ultrafine particles cannot be explained by classical homogeneous nucleation theory, but is reproduced in detail by a microphysical simulation when including CI emissions (sum of positive and negative ions) of 2.6×10^{17} per kg of fuel [*Kärcher et al.*, 1998b; *Yu et al.*, 1998]. The model explains the measured bimodal size spectrum with enhanced coagulation by charged particles [*Yu and Turco*, 1997]. The mode above 14 nm results from quickly growing charged particles, while only a few of the neutral particles grow to the detected size of >5 nm diameter. For high FSC the volatile material is consistent with a fuel sulfur to H$_2$SO$_4$ conversion fraction ε of 1.8%. For low FSC (22 µg/g) an unrealistically high conversion of 55% would be required to explain the volatile material measured. It was suggested that part of the volatile material results from condensable exhaust hydrocarbons. Further support for this conclusion was given in a follow-up study by *Yu et al.* [1999].

[34] Total sulfuric acid (gas plus aerosol) concentrations from engine exhaust was for the first time directly measured in the exhaust plume of a jet aircraft in flight with the Volatile Aerosols Component Analyzer (VACA) [*Curtius et al.*, 1998; *Curtius and Arnold*, 2001]. The instrument consists of a backward facing sample inlet, a heated flow tube (90°–120°C), an ion source injecting nitrate ions to chemically ionize sulfuric acid, and a quadrupole mass spectrometer to detect the ions. The heater evaporates the volatile components of small aerosol particles entering the instrument. The detection limit for H$_2$SO$_4$ concentration is 10^7 cm^{-3}. Owing to a number of loss processes, the obtained H$_2$SO$_4$ concentrations are regarded as lower-limit values. The measurements were verified during a first flight by injecting sulfuric acid directly into the exhaust jet at engine exit and measuring it in the aged plume. The mass spectra obtained in the exhaust of sulfur-poor fuel during the second S5 flight did not differ from the background spectra showing only the reactant ions NO$_3^-$ (HNO$_3$)$_m$ with $m = 0$ and 1. However, for the sulfur-rich fuel the spectra show clear signatures of sulfuric acid: HSO$_4^-$, HSO$_4^-$ (HNO$_3$), and HSO$_4^-$ (H$_2$SO$_4$), at 97, 160, and 195 amu, respectively. The H$_2$SO$_4$ concentration reached values as high as 1500 pmol mol^{-1} (background: 10–50 pmol mol^{-1}) and was closely correlated with increases of temperature and CO$_2$ mixing ratio, see Figure 2. A conversion fraction
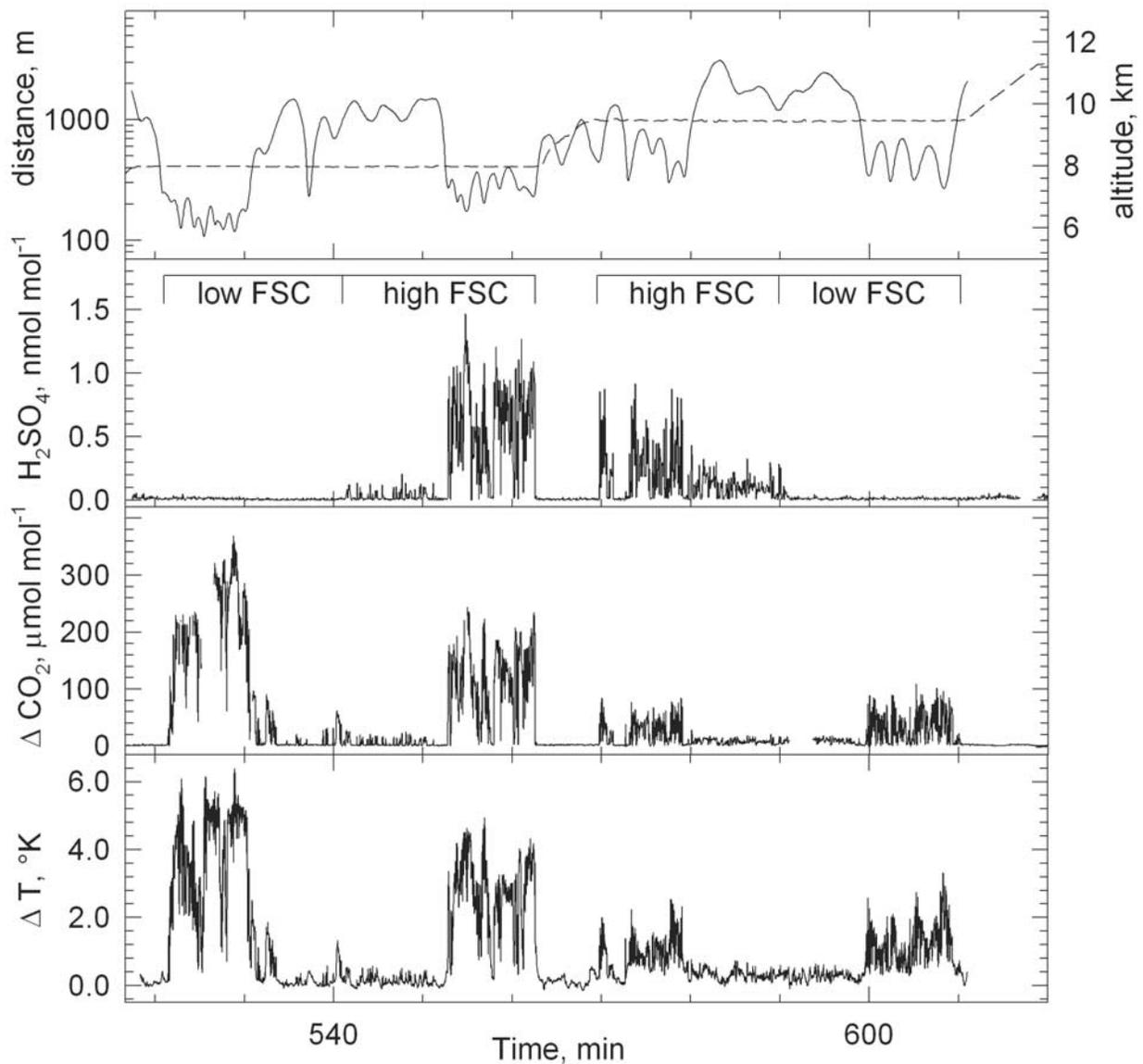
Figure 2. First measurements of sulfuric acid concentration and the conversion fraction ε of fuel sulfur into sulfuric acid in the engine exhaust gases of a jet aircraft at cruise during SULFUR 5 by VACA [*Curtius et al.*, 1998]. During flights of the Falcon at 8 to 10 km altitude, 70 to 300 m behind the ATTAS, clear increases in carbon dioxide ($\Delta CO_2 \approx 200$ μmol mol^{-1}) and temperature ($\Delta T \approx 3.5$ K) were measured in the exhaust plume. The temperature and CO_2 increases imply dilution factors N (amount of exhaust mass per unit mass of burned fuel) of $N \approx 10^4$ for the given example, which is consistent with the dilution law $N(t) = 7000$ $(t/t_0)^{0.8}$, $t_0 = 1$ s, for a plume age t of 1.6 s [*Schumann et al.*, 1998]. When the ATTAS was burning fuels with high fuel sulfur content (FSC = 2700 μg/g), the measurements show clearly correlated increases in sulfuric acid ($\Delta H_2SO_4 \approx 1$ nmol mol^{-1}). The ratio of signals implies $\varepsilon = (\Delta H_2SO_4/\Delta CO_2)$ (32/44) EI$_{CO2}$/FSC $\approx 0.4\%$ (32/44 is the ratio of molar masses of S and CO_2). Because of potential wall losses within the instrument and the inlet, this value represents a lower bound to the actual conversion fraction. No increase in ΔH_2SO_4 was detectable when the ATTAS engines were burning fuel with low FSC (22 $\pm$ 5 μg/g). Taking into account background fluctuations and statistical scatter, the conversion fraction at low FSC cannot be larger than 2.5 times the value at high FSC.

of fuel sulfur to H_2SO_4 of at least 0.34% was deduced from these data [*Curtius et al.*, 1998].

[35] If the conversion fraction would be the same for the low as for the high FSC, the expected increase is below 12 pmol mol^{-1} even for very young plume ages. During penetrations of the sulfur-poor plume the sulfuric acid concentration did not increase significantly above the local atmospheric background level of 15 to 50 pmol mol^{-1}. A

signal should have been visible if the conversion fraction at low FSC would be 2.5 times larger than at high FSC. Hence the conversion rate at low FSC was <2.5 the value at high FSC [*Curtius et al.*, 1998]. If the upper bound for ε is 1.8% at high FSC, as inferred from matching the measured aerosol number concentrations with $d > 5$ nm and $d > 14$ nm with aerosol models including CIs [*Yu and Turco*, 1998a; *Kärcher et al.*, 1998b; *Yu et al.*, 1998], an upper bound at low FSC for the ATTAS is 4.5%. This value is not far off the value 6% computed by *Brown et al.* [1996b] for the ATTAS engines at low FSC.

[36] In the first S5 flight a further instrument (Large Ion-Mass Spectrometer, LIOMAS) was flown on the Falcon to measure gaseous negative ions in the exhaust plume of the ATTAS jet aircraft in flight [*Arnold et al.*, 1999]. It was found that by far most of the negative ions had mass numbers >450 amu and number densities which markedly exceeded the number densities of ambient atmospheric ions. The large concentrations measured suggest that the massive ions observed inside the plume originated from CIs in the jet engines. The results for the low FSC suggest that the massive ions consist at least partly of species other than sulfuric acid. The measured number density of ions decreased faster than expected from dilution. A total negative ion concentration of $>5 \times 10^4$ cm^{-3} for a plume age of 1 s was inferred. The measured data represent lower bounds due to partial losses of the ions on the walls of the sampling tubes, and from the growth of charged particles beyond the size detectable by the instrument [*Arnold et al.*, 1999; *Wohlfrom et al.*, 2000].

3.6. Ultrafine Particle and Ion Composition and Size Distribution During SULFUR 6

[37] The previous measurements provided much progress in identifying the number of ultrafine particles, but the size spectrum of particles was still poorly defined because of missing continuity from the smallest clusters to the particles which can be measured optically at sizes of ~100 nm and larger. Moreover, first measurements with a new LIOMAS instrument revealed surprisingly large ions in the exhaust plume of the DC8 (0.5 to 1.5 s plume age) during the POLINAT 2 experiment. Gaseous H_2SO_4 was additionally detected by SIOMAS in the exhaust plume of the DC8 (about 3×10^9 cm^{-3} at 1 s plume age), possibly because of the smaller plume age compared to the A310 case (details to be described elsewhere).

[38] Therefore S6 was performed. The measuring concept remained basically unchanged compared to S5. However, the alternatively operating heating section of the CPCs ($d > 14$ nm) was replaced by a parallel monitoring of the nonvolatile aerosol fraction with $d > 10$ nm and great effort was spent to achieve a more detailed size resolution for nuclei and Aitken mode aerosols. Furthermore, a soot photometer and a nephelometer were integrated for an independent determination of the aerosol absorption and scattering coefficients. The FSSP-300 was modified for the detection of ice crystal concentrations larger than 5000 cm^{-3} by additional monitoring of the probe's electronic "activity" to determine and correct for the actual dead time fraction during the measurement [*Schröder et al.*, 2000a]. For the first time the particle size distributions from 3 to 60 nm diameter were determined using an extended set of 10 CPCs

operated in parallel with successively increasing lower size detection limits (Table 2). By normalization with simultaneously measured CO_2 concentrations an apparent particle emission index (PEI) was determined [*Brock et al.*, 2000; *Schröder et al.*, 2000b]. Moreover, an improved LIOMAS instrument with increased mass range (1–8500 amu) [*Wohlfrom et al.*, 2000] and an improved VACA instrument were provided with reduced surfaces in the internal heating system reducing possible wall losses, and the instrument was calibrated with sulfuric acid/water aerosol particles in the laboratory [*Curtius and Arnold*, 2001].

[39] In situ measurements were performed at cruise altitudes behind the ATTAS and a B737 aircraft. Measurements were made 0.15–20 s after emissions as the source aircraft burned fuel with various FSCs, see Table 4. Measurements of ultrafine aerosol particles showed that nonsoot particles were present in high concentrations [*Schröder et al.*, 2000b; *Brock et al.*, 2000]. The actually detected numbers of particles formed correspond to particle EIs exceeding 1×10^{17} kg^{-1} and 2×10^{16} kg^{-1} for particles >3 nm and >5 nm, respectively. Consequently, the true concentrations of volatile aerosols (including the fraction below 3 nm) were estimated to exceed 2×10^{17} kg^{-1}. Volatile particle emissions did not change significantly with FSC when FSC was reduced below 100 μg/g. The measured particle emissions increase with plume age. The particle number concentrations are much smaller (by about a factor 4–8) in plumes at ambient conditions where contrails form than in plumes without contrails. The experiments give again clear indications that nonsulfate compounds, most likely condensable hydrocarbons, begin to dominate the volatile particle composition as FSC decreases below about 100 μg/g. The EI for volatile particles is only weakly dependent on the engine type.

[40] In addition to the results of S4 and S5, S6 was used to determine the emissions of soot (nonvolatile particles) from the ATTAS, the A310, and the B737 [*Petzold et al.*, 1999]. Soot number densities varied from 3.5×10^{14} (B737) to 1.7×10^{15} kg^{-1} (ATTAS), with corresponding mass EIs of 0.011 g kg^{-1} to 0.1 g kg^{-1}. The combination of soot photometer and integrating nephelometer showed an aerosol single-scattering albedo of about 1 outside the plume and <0.01 inside the plume which clearly indicated that by far the largest fraction of emitted particles is composed of black carbon. Additionally, the soot photometer for the first time provided a direct in-flight measurement of the emitted soot mass which agreed very well with soot mass concentrations calculated from measured size distributions [*Petzold et al.*, 1999].

[41] A new correlation method was set up to estimate the mass EIs based on available ground measurements. The measured and computed values agree within about 10% at cruise conditions. The correlation method was used to estimate the mean EI of soot by the globally operating aircraft fleet of 1992 to be 0.038 g kg^{-1} [*Petzold et al.*, 1999].

[42] Ice crystal concentrations inside young contrails were measured with the improved FSSP-300 to reach 4×10^4 cm^{-3} and $8–10 \times 10^4$ cm^{-3} for the B737 (plume age 0.4 s, FSC = 2.6 μg/g) and the ATTAS (1 and 20 s, 2.6 and 118 μg/g). The results were confirmed by extrapolation of measurements carried out at larger distances and correspond

to PEIs of $3.6 \times$ and 15×10^{14} kg^{-1} with about 50% uncertainty.

[43] Total sulfuric acid concentrations were measured behind the B737 with the mass spectrometer instrument VACA in the very young plume (>0.15 s). Unfortunately, the upper FSC values of the fuels provided at Munich airport (56 µg/g) were rather small. Sulfuric acid (up to 8×10^9 cm^{-3} or about 600 pmol mol^{-1}) produced from fuel sulfur was detected when the engines burned fuel with FSC = 56 µg/g, but for the extremely low FSC = 2.6 µg/g a slightly enhanced (with respect to the background) H_2SO_4 concentration was registered only at the shortest distance. From the simultaneous CO_2 and H_2SO_4 measurements a conversion fraction of fuel sulfur to H_2SO_4 of $\varepsilon = 3.3 \pm 1.8\%$ was deduced for the case of FSC = 56 µg/g [*Curtius et al.*, 2002]. The ε value is larger than the lower limit ε of 0.34% for the ATTAS, possibly because of the different engine (see below). However, the larger value also results because of reduced and calibration-corrected inlet wall losses. This is the first absolute and direct measurement of the conversion fraction of fuel sulfur in the exhaust plume of an aircraft. The direct method is considered to give results which are more reliable than those derived indirectly from aerosol data.

[44] For comparison, if the volatile aerosol contains only H_2SO_4 and H_2O, *Brock et al.* [2000] derived $2.4 \pm 0.8\%$ conversion from the aerosol size distribution in the diameter range 3 to 10 nm at plume ages 0.4 to 0.6 s. On the basis of observed growth of particles with plume age they expected 2–3 times larger values in the mature plume. An analysis of the CPC data with the model by *Kärcher et al.* [2000] (described below) suggests even larger (factor 10) increases in aerosol volume by 3 s plume age, so that this cannot be used to derive a realistic upper limit for ε.

[45] Both negative and positive CIs were measured by LIOMAS in flight in the plume of the ATTAS at plume ages of 0.6 and 6.2 s [*Wohlfrom et al.*, 2000]. Massive ions were detected with a quadrupole mass spectrometer of high sensitivity and low mass discrimination. It is operated in an integral high-pass mode where all ions above a lower cutoff mass pass the quadrupole rod system and are detected by a channel electron multiplier; scanning the cutoff mass results in an integral mass spectrum. CI mass distributions were obtained for mass numbers up to 8500 amu, and additionally the total number of CIs exceeding this size limit was determined.

[46] Both positive and negative CIs were found to be very massive even when nearly sulfur-free fuel was burned in the ATTAS engines (FSC of 2 µg/g). Observed positive CIs have a smaller mean mass compared to negative CIs. The raw CI data are CI counts in arbitrary units. The data were normalized to fit the size spectra derived from the CPC counters, see Figure 3. The normalized CI data extend the particle size spectra into the range below 3 nm, the presently lowest detectable particle size for CPCs. The spectral shape of the particle distributions measured by CPCs [*Schröder et al.*, 2000b] and detected by the IOMAS [*Wohlfrom et al.*, 2000] for the first time resolve the main mode position close to 3 nm diameter. The positive CI concentrations have a maximum near $d = 1.5$ nm. The size distribution of positive ions was similar for two FSC values (2 and 118 µg/g), while the size distribution of the negative CIs was shifted toward

larger sizes. For FSC = 118 µg/g a significant number of the ion population seems to be larger than 2.8 nm [*Wohlfrom et al.*, 2000]. Similar behavior was modeled in detailed numerical simulations [*Yu et al.*, 1999]. In ground-based measurements, no significant CI-growth was observed when the FSC was raised from 2 to 66 µg/g [*Kiendler et al.*, 2001]. Hence, whereas the positive CIs do not grow strongly from sulfur but more likely from low volatility hydrocarbons, the negative CIs do grow with increasing FSC. CIs are present also in the size range measured with CPCs.

[47] Composition measurements of negative and positive CIs were made by a novel quadrupole ion trap mass spectrometer. Measurements were taken behind the ATTAS and other jet engines at ground and over a kerosene burner flame in the laboratory by *Kiendler et al.* [2000a, 2000b]. Unambiguous mass determination and identification of the chemical nature of ions were performed. The measurements indicate that sulfuric acid does not tend to strongly condense on positive ions and that positive ions in aircraft jet engine exhaust contain preferably organic molecules [*Kiendler et al.*, 2000b]. This is consistent with model assumptions [*Yu et al.*, 1999].

[48] Total positive CI concentrations in the ATTAS engine exhaust at the ground were measured [*Arnold et al.*, 2000] using an electrostatic probe (Gerdien-condenser). For a plume age of 12 ms, 1.4 m behind the engine exit, the positive ion concentration was 1.6×10^8 cm^{-3}. The number of positive ions decreases rapidly with increasing plume age, but is independent of FSC. When both ion-ion recombination and plume dilution are taken into account, it seems that the initial ion concentration at the engine exit plane is about 1×10^9 cm^{-3}, corresponding to a CI number EI of about 10^{17} kg^{-1} [*Arnold et al.*, 2000]. A more detailed model analysis by *Sorokin and Mirabel* [2001] finds for the same data a maximum concentration for the positive and negative ions at engine exit at ground of 0.8×10^9 cm^{-3} with an uncertainty of $\pm 30\%$, which is not essentially different from the above 1×10^9 cm^{-3}. One should note that the ion concentration is likely to be much larger at combustor exit than at engine exit [*Starik et al.*, 2002].

3.7. Engine Technology Influence on Contrails and Particles in SULFUR 7

[49] The most recent S7 experiment was performed to test the influence of engine efficiency on contrail formation. Such an influence was expected based on S1 and in the meantime deduced from many individual contrail observations during POLINAT and SUCCESS [*Jensen et al.*, 1998a; *Kärcher et al.*, 1998a; *Schumann*, 2000], but direct evidence for different contrail formation from two aircraft with different engine efficiencies was missing. In the experiment, contrail formation was observed behind two four-engine jet aircraft with different engines flying wing by wing. The two contrail forming aircraft were a Boeing B707 and an Airbus A340. The two aircraft were selected for this test because the modern A340 engines provide significantly higher engine efficiency than those of the older B707 with lower bypass and pressure ratio, see Table 3. An altitude range exists, see Figure 1d, in which the aircraft with high engine efficiency causes contrails, while the other aircraft with lower engine efficiency causes none [*Schumann et al.*,
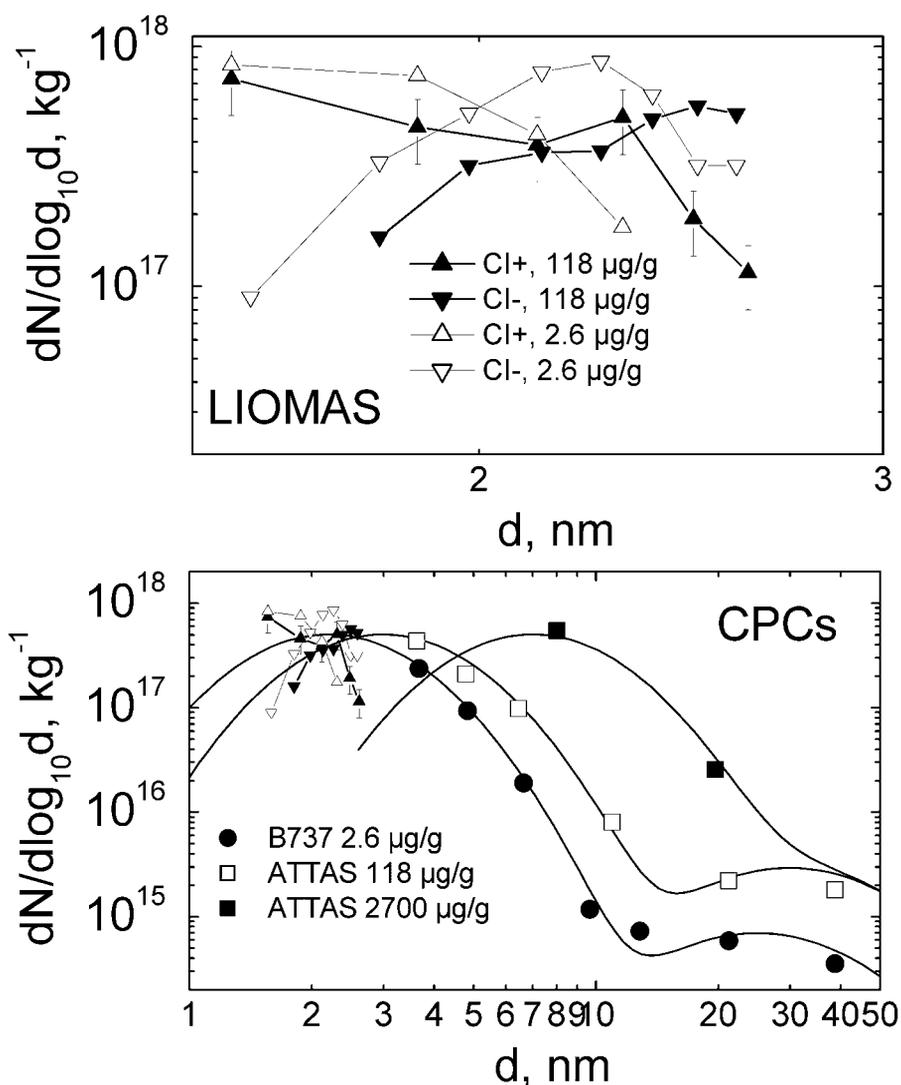
Figure 3. Number size distributions of CIs per unit mass of fuel burned (top and bottom panel) as obtained with LIOMAS behind the ATTAS during SULFUR 6 [*Wohlfrom et al.*, 2000] and plume aerosol particles (bottom panel) measured with CPCs during SULFUR 5 and 6 [*Schröder et al.*, 2000b] for different FSCs. The three bimodal distributions (bottom panel) represent parameterizations of measurements behind the B737 (2.6 µg/g FSC) and the ATTAS (118 and 2700 µg/g FSC). The CI data are for 2.6 and 118 µg/g FSC (open and solid symbols) for positive (triangle upward) and negative ions (triangle downward). The mass bins of the spectrometric measurements were converted to particle diameters assuming spherical particles with density 1.4 g cm^{-3}. It should be noted that the LIOMAS does not detect any neutral particles which may have been formed via recombination of positive and negative ions in the very young exhaust plume, and provides normalized spectra only. Therefore the LIOMAS data have been normalized to fit the aerosol data assuming a total number of particles (CIs of either sign and CNs) corresponding to a particle emission index of 2.0 and 2.4 × 10^{17} kg^{-1} for 2.6 and 118 µg/g FSC, respectively.

2000b]. Table 4 shows that all contrails were observed in close accordance with the Schmidt/Appleman criterion.

[50] The aerosol measurements in the young plumes of the A340 (Table 4, near flight level 314) and B707 (310) with typical FSC values (380 and 120 µg/g) and at non-contrail-forming conditions, at close separation (70 to 140 m; determined from photos, see Figure 1f) reveal strong differences, see Figure 4. The number of nonvolatile (mainly soot) particle emissions is about 1 order of magnitude larger for the B707 than for the A340, see Table 6. The data in this table are based on events with peak plume concentrations (12–15 in number) inside the young plume, with typically ±30% uncertainty. The volume size spectrum of the B707 is dominated by particles measured with the
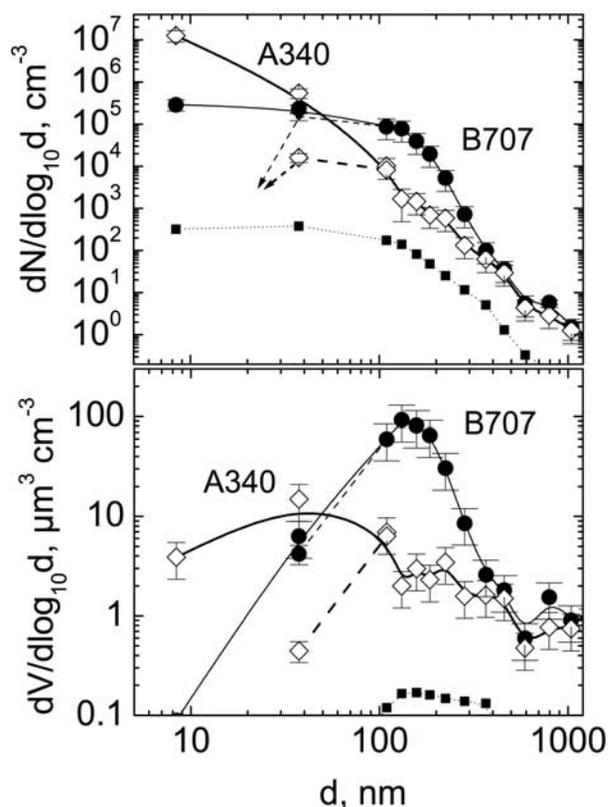
Figure 4. Number density data of total aerosol interpolated with straight lines (top) and volume density data of nonvolatile aerosol fitted by bimodal long-normal distributions (bottom) versus particle diameter d of jet exhaust aerosol under noncontrail-forming conditions for the B707 (solid curves, solid circles) and the A340 (dashed curves, open circles) aircraft during SULFUR 7, and in the background atmosphere (dotted curve, solid diamonds). For $d > 100$ nm the results are from the PCASP wing station (assuming refraction indices of black carbon for the plume aerosol and polystyrene latex spheres for the background aerosol). The data at 8 nm (5–14 nm range) and near 16 to 30 nm (14–110 nm range) are based on CPC measurements without heating (top) or after heating to 500 K (bottom). Note that for $d < 100$ nm, S7 provided far less size resolution than S6.

PCASP. The optical properties of the particles and the volume spectra are derived assuming spherical soot particles which may be debatable. The soot mass EIs determined from these data, see Table 7, show a trend toward less soot emissions with more modern engine technology. The number of volatile particle emissions detected with diameter >5 nm (the majority concentrated in the nuclei mode range) differed even more and in the opposite way, see Figure 4 and Table 6. The surface and volume densities differ also strongly, see Table 6. The available aerosol surface area in the young, noncontrail plume is bound to the lower accumulation mode range around 100 nm diameter for the B707 case but widely shifted into the Aitken mode (~50 nm) for the A340-case. The PEI for the A340 are about 10 times larger than for the B707, see Table 8. The differences in the engines go along with differences in the EIs for CO which we measured during these flights: A340, 1.9 g kg^{-1}; B707, 14.4 g kg^{-1}. While the old engines emit more aerosols by mass, the modern engines contribute a larger number of (ultrafine) particles.

[51] If one would assume that the volatile material is composed of sulfuric acid and water only, a volume density v of volatile aerosol (Table 6) would imply a conversion fraction $\varepsilon^* = \rho_{acid} v \, x_{acid} \, N \, 32/(98 \, \text{FSC} \, \rho)$, with acid density $\rho_{acid} = 1.8$ g cm^{-3}, acid mass fraction $x_{acid} = 0.92$, air density ρ, and dilution factor $N = 5000$. This yields $\varepsilon^* = 1.6$, 22, and 25% for the A340 and 0.4, 21, and >100% for the B707, depending on whether one computes the volume just from the numbers of volatile particles counted with the CPCs and their cutoff diameters of 5 and 14 nm, or takes the values derived from the volume distribution as listed in Table 6 without or with the volume measured with the PCASP. The maximum values are clearly unrealistic. These considerations show the large uncertainty range of such estimates.

[52] The in-flight measurements in the wakes of the A340 and B707 aircraft with the LIOMAS instrument confirmed that already 70 to 140 m behind the engine, 50–60% of the negative CIs formed during combustion have grown to masses of more than 8500 amu, in particular for the A340.

4. Discussion
4.1. Fuel Sulfur to Sulfuric Acid Conversion Fraction

[53] Conversion fractions ε (per molecule) derived from the SULFUR experiments, as well as from SUCCESS

Table 6. Aerosol Concentrations in the Young Plume Behind the A340 and B707 Aircraft During S7, and in the Background Upper Troposphere

Aerosol Data[a]	Unit	A340	B707	Background
Total Aerosols				
Number $d > 5$ nm	cm^{-3}	4×10^6	3×10^5	500
Number $d > 14$ nm	cm^{-3}	5×10^5	2×10^5	420
Surface	μm^2 cm^{-3}	3000 (70)	1900 (1100)	5
Volume	μm^3 cm^{-3}	15 (2)	32(28)	0.2
Nonvolatile Particles				
Number $d > 10$ nm	cm^{-3}	0.15×10^5	1.5×10^5	<50

[a]Concentrations per unit volume; numbers in parentheses denote the contributions from particles measured with the PCASP; estimated plume age 0.4 to 0.8 s; concentrations are given for plume conditions with dilution factor 5000, based on temperature and humidity increases measured in the plume. The uncertainty is typically ±30%. The total number concentration of particles with $d > 5$ nm behind the A340 may reach as high as 10^7 cm^{-3} because the CPC counter of type TSI 3760A used was close to saturation (coincidence correction included).

Table 7. Soot Mass and Number Emission Indices at Cruise and Smoke Numbers[a]

Aircraft	EI_{soot}, g kg^{-1}	PEI_{soot}, 10^{15} kg^{-1}	SN at 100%	SN at 30%
B707	0.5 ± 0.1	1.7 ± 0.3	54.5	n.a.
ATTAS	0.1 ± 0.02	1.7 ± 0.35	46.3	10.9
A310	0.019 ± 0.01	0.6 ± 0.12	5.8	n.a.
B737	0.011 ± 0.005	0.35 ± 0.07	4	2.5
B747		0.27, 0.45	16.0	n.a.
DC10		0.46	11.4	1.6
A340	0.01 ± 0.003	0.18 ± 0.05	12.6	1.0

[a]EI_{soot} and PEI_{soot}: soot mass and number emission indices per unit mass of fuel burned; smoke number (SN) at two power settings from *ICAO* [1995] as far as available; data for ATTAS, A310, and B737 from *Petzold et al.* [1999]; for B747 and DC10 from measurements performed by the University of Missouri-Rolla [*Schumann et al.*, 2000a]; B707 and A340 from this work. EI_{soot} values are derived by fitting bimodal lognormal distributions to the PCASP and the nonvolatile CPC data, see Figure 4 [*Petzold et al.*, 1999].

(measurements behind a B757 [*Miake-Lye et al.*, 1998]), the Concorde [*Fahey et al.*, 1995], from the Lufthansa ground test facility [*Frenzel and Arnold*, 1994], and from POLINAT 2 [*Schumann et al.*, 2000a] are compiled in Table 8. The table collects the data for different lower cutoff sizes of the particle counters, plume ages from 0.15 to 3360 s, FSC values from 2.6 to 5500 μg/g, different instrument techniques, different methods to indirectly derive ε values, and various aircraft/engine combinations at cruise or at ground. The table extends a similar one of *Brock et al.* [2000].

[54] The only direct measurements of sulfuric acid in the exhaust plume of cruising aircraft are those obtained for the ATTAS and B737 aircraft. The measurements behind the ATTAS reveal a conversion of fuel sulfur to sulfuric acid with fraction ε > 0.34% [*Curtius et al.*, 1998], consistent with direct measurements at ground during S3 (ε = 1.2%, at FSC of 212 μg/g) [*Arnold et al.*, 1998a], and in accordance with the early result (ε > 0.4%) measured at ground by *Frenzel and Arnold* [1994]. The amount of volatile material found at high FSC suggests ε < 1.8% [*Yu and Turco*, 1998a; *Kärcher et al.*, 1998b; *Yu et al.*, 1998], and the combined VACA/CPC findings imply ε < 4.5% at low FSC for the ATTAS. For the B737, ε is measured to be 3.3 ± 1.8% for the rather low FSC of 56 μg/g [*Curtius et al.*, 2002].

[55] Otherwise, the listed apparent ε values (denoted by ε*) are derived from volatile particle volume measurements in the young exhaust plume for various FSC values. For low FSC values some of the results imply ε* > 50%. The low-sulfur aerosol data measured behind the ATTAS would imply even larger ε* fractions than derived elsewhere, and the results for the B707 and A340 are within the same range as the SUCCESS results [*Toon and Miake-Lye*, 1998]. Such large conversion efficiencies cannot be explained by sulfuric acid formation with model computations for reasonable engine emissions [*Brown et al.*, 1996b; *Lukachko et al.*, 1998; *Tremmel and Schumann*, 1999; *Miake-Lye et al.*, 2001; *Starik et al.*, 2002], nor are they consistent with measurements at the ground [*Arnold et al.*, 1998a; *Hunton et al.*, 2000]. The aerosol-derived ε* depends strongly on the cutoff diameter *d* above which more than 50% of the particles are counted; on possibly an enhanced counting efficiency for charged clusters; on the width of the detector size sensitivity, in particular for small *d*; on the shape of the aerosol number spectrum which folds with the detector sensitivity function; on wall losses of small or very large particles in the inlet [*Cofer et al.*, 1998], possibly with

enhanced wall losses for charged particles; and on enrichment effects due to nonisokinetic sampling of ice particle residuals. A 21% uncertainty in *d*, which may be expected [*Wilson et al.*, 1983; *Brock et al.*, 2000; *Schröder et al.*, 2000b], implies 50% uncertainty in ε*. Variations in the particle counter sensitivity and aerosol spectrum may cause up to 50% uncertainty in ε* for *d* < 10 nm if not carefully corrected [*Brock et al.*, 2000]. The detection sensitivity of a CPC to charged molecule clusters is unknown [*Yu and Turco*, 1998b]. A large enrichment of residuals from ice crystals larger than about 1 μm cannot be excluded if forward looking aerosol inlets are used [*Konopka et al.*, 1997]. For the same reason, the interstitial aerosol inlet does not count the volatile aerosol contained in contrail ice particles [*Schröder et al.*, 2000b]. *Brock et al.* [2000] concluded a relative uncertainty of ±38% for the ε* values derived for the B737 at FSC = 56 μg/g, including uncertainties in FSC. Otherwise, it must be assumed that much of the scatter in the reported ε* values is due to uncertainties mainly with respect to particle composition.

[56] The strong increase in the aerosol derived ε* for small FSC values indicates that condensable gases other than sulfuric acid contribute to the formation of volatile particles in the young exhaust plume, as originally suggested by us during the panel discussion at the International Colloquium "Impact of Aircraft Emissions Upon the Atmosphere," Office National d'Etudes et de Recherches Aérospatial (ONERA), Chatillon, Paris, 15–18 October 1996. The conjecture was introduced to offer an explanation for the large fuel sulfur conversion fraction ε reported by *Fahey et al.* [1995] from the Concorde measurements. These measurements could be explained only under the assumption that a large fraction of the fuel sulfur (25 to 60%) is converted to S^{VI} (H_2SO_4 + SO_3), already before leaving the engine exit [*Danilin et al.*, 1997; *Kärcher and Fahey*, 1997; *Yu and Turco*, 1998b]. Alternative explanations in terms of CIs [*Yu and Turco*, 1997, 1998b] or oxidation to S^{VI} in the plume by some "unknown" chemistry [*Danilin et al.*, 1997] could not explain the large amount of volatile material found behind the Concorde and in young exhaust plumes. In view of measured OH concentrations formed in the plume mainly by photolysis of nitrous acid [*Hanisco et al.*, 1997] and new laboratory studies, major sulfur oxidation in the aging plume can be excluded [*Rattigan et al.*, 2000]. An effort performed by *Konopka et al.* [1997] to deduce the sulfuric acid content in volatile particles from the measured particle size spectra

Table 8. Conversion Fraction of Fuel Sulfur to Sulfuric Acid and Particle Number Emission Indices From Various Studies[a]

FSC, μg g⁻¹	Aircraft	Engine	Experiment, Conditions	Technique	Plume Age, s	ε, %	d, nm	PEI$_{soot}$, 10^{15} kg⁻¹	PEI$_{total}$, 10^{15} kg⁻¹	Reference
2.6	B737	CFM56-3B1	S6, no contrail	CPC	0.2–0.6	>17 ± 6[b]	3	0.35	60	Brock et al. [2000], Schröder et al. [2000b]
	ATTAS	Mk501		CPC	0.5–7	>20–80[b]	4	1.8	100	Schröder [2000], Schröder et al. [2000b]
20	ATTAS	Mk501	S5, no contrail	CPC/model	0.8–10	>55[b]	5	1.7	5–20	Kärcher et al. [1998b], Yu et al. [1998]
				H₂SO₄-CIMS	>0.5	0.34 < ε <4.5[b]	...	...	...	Curtius et al. [1998], this work
56	B737	CFM56-3B1	S6, no contrail	CPC	0.2–0.6	>2.4 ± 0.8[b]	3	0.35	90	Brock et al. [2000], Schröder et al. [2000b]
				H₂SO₄-CIMS	>0.15	3.3 ± 1.8	...	...	...	Curtius et al. [2002]
72	B757	RB211	SUCCESS, contrail	CPC	0.2–80	8 ± 3[b]	4	0.2–0.9	1–2	Miake-Lye et al. [1998]
				SO₂-CIMS	0.2–80	6 (0–34)	...	...	...	Miake-Lye et al. [1998]
				CPC		8[b]	4	0.6 ± 0.1	1.4 (0.8–2)[c]	Anderson et al. [1998b]
				DMA	10–100	19[b]	8	0.07[c]	0.28[c]	Hagen et al. [1998]
				impactor		37[b]	20	0.17[c]	...	Pueschel et al. [1998]
118	ATTAS	Mk501	S6, no contrail	CPC	>0.5	2.3[b]	3	1.8	150	Schröder et al. [2000b]
120	B707	JT3D-3B	S7, no contrail	CPC	0.4–0.7	(0.4–21)[b]	5	1.7	6	this work
170	ATTAS	Mk501	S2, contrail	CPC/model	20	(0.4–1.8)[b]	7		8	Schumann et al. [1996], Yu and Turco [1998a]
212	ATTAS	Mk501	S3, ground	CIMS (IOMAS)	0.0066	1.2	...	...	...	Arnold et al. [1998a]
230	Concorde	Olympus 593	Mach 2, no contrail	CPC	780–3360	>12,[b] >46[b]	9	43–87	17–650	Fahey et al. [1995]
				impactor	1107–1708		50	0.008[c]		Pueschel et al. [1997]
240	B747		POLINAT	DMA	84–90	0.4–21.7[b]	12	0.54	3.5	Konopka et al. [1997]
260	B747		POLINAT	DMA	119	1.1–40.7[b]	12	0.46	8.4	Konopka et al. [1997]
265	DC10		POLINAT	DMA	76–88	0.9–36.8[b]	12	0.27	10.1	Konopka et al. [1997]
380	A340	CFM56-5C4	S7, no contrail	CPC	0.5–0.8	(1.6–22)[b]	5	0.18	48 (32–100)	this work
480	A340	CFM 56-2C1	POLINAT 2, contrail	CPC	100		5	1.6	19–23	Schumann et al. [2000a]
676	B757	RB211	SUCCESS, contrail	CPC	0.2–80	>15 (±7)[b]	4	0.2–0.9	10–100	Miake-Lye et al. [1998]
				SO₂-CIMS	0.2–80	31 (15–52)	...	...	...	Miake-Lye et al. [1998]
				CPC		15[b]	4	0.5 ± 0.2	15 (4–40)	Anderson et al. [1998b]
				DMA	10–100	26[b]	8	0.28[c]	2.6 ± 0.4[c]	Hagen et al. [1998]
				impactor		10–26[b]	20	0.7–5.2[c]	...	Pueschel et al. [1998]
690	DC8	CFM 56-2-C1	POLINAT 2, contrail	DMA	1–5	...	7	0.011[c]	...	Paladino et al. [2000]
1000	...	modern engine	LH test site Hamburg	CIMS (IOMAS)	0.2	>0.4	...	...	...	Frenzel and Arnold [1994]
2700	ATTAS	Mk501	S5, no contrail	CPC	>0.5	1.8[b]	5	1.7	200	Kärcher et al. [1998b], Yu et al. [1998]
				H₂SO₄-CIMS	>0.5	0.34 < ε <1.8[b]	...	...	...	Curtius et al. [1998], this work
5500	ATTAS	Mk501	S2, contrail	CPC + models	20	(0.4–1.8)[b]	7	...	10	Schumann et al. [1996], Yu and Turco [1998a]

[a]The table is ordered by fuel sulfur content (FSC); ε = conversion mole fraction, d = cutoff diameter, PEI$_{soot}$ and PEI$_{total}$ = particle number emission indices of nonvolatile or ''soot'' particles and total (including volatile) particles per unit mass of fuel burned. Values in parentheses denote the possible range of results from the experiments.

[b]Calculated from particulate volume and presuming that the particles are exclusively composed of sulfuric acid and water, denoted by epsilon star in the text.

[c]The values derived from DMA and impactor instruments deviate from the CPC data, possibly because of inlet wall losses, other cutoff sizes, or smaller collection efficiency.

Table 9. Computed Engine Parameters and Conversion Fractions ε Compared to Measurements

Aircraft	Engine[a]	Flight Level, hft	Combustor Exit Teperature, K	Combustor Exit Pressure, hPa	Age at Engine Exit, ms	Temperature at Engine Exit, K	Pressure at Engine Exit, hPa	ε, %, Computed	ε, %, Measured
ATTAS	Mk501	310	1154	5243	5.2	581	288	3.4	0.4–4.5
ATTAS	Mk501	260	1154	5727	5.4	599	360	3.7	0.4–4.5
B737	CFM56	350	1237	6050	6.5	544	238	5.9	3.3 ± 1.8
B737	CFM56	260	1209	5987	7.5	592	360	5.6	3.3 ± 1.8
B747	RB 211	350	1540	11,000	4.6	598	220	9.6	…

[a]Cases ATTAS and B737 from G. Tremmel (personal communication, 1999); case B747 from *Starik et al.* [2002].

obtained during POLINAT indicated that even 100% conversion from fuel sulfur would not suffice to explain the measured volume of volatile material in exhaust aerosols in some cases, but oversampling of ice particles containing volatile particles could not be excluded. These discussions motivated studies to look for low volatility hydrocarbons, possibly including aldehydes, alkenes, and alkynes [*Kärcher et al.*, 1998b; *Yu et al.*, 1999]. Organic material was measured in soot by *Petzold and Schröder* [1998]. Evidence for the existence of organic material clusters in the exhaust is provided by "OHC ions" containing C and H atoms and in part also O atoms in negative CIs measured by *Kiendler et al.* [2000a].

[57] Engine chemistry models imply a decrease of ε with growing FSC because of the finite amount of oxidizing radicals available at the combustor exit. For the ATTAS engine, *Brown et al.* [1996b] computed ε = 6 % and 1% for FSC = 2 and 5400 μg/g, very close to the upper limits derived for ε in the present paper. Other studies [*Lukachko et al.*, 1998; *Tremmel and Schumann*, 1999; *Starik et al.*, 2002] deduced a weaker dependence on FSC. Most volatile aerosol data suggest a strong decrease of ε^* with increasing FSC, but this may be misleading because of possible organic components. The increase in conversion fraction with FSC derived from SO_2, CO_2, and FSC data [*Miake-Lye et al.*, 1998] is likely an artifact due to problems in measuring the FSC, and the precision of the SO_2 and CO_2 data does not allow to determine the nonmeasured S^{VI} fraction as a remainder for conversion fraction values below 10 to 20% [*Hunton et al.*, 2000].

[58] The ATTAS ε^* values of 55 and 1.8% for 20 and 2700 μg/g FSC could be unified with ε^* of 1.4% and 40 μg/g emitted condensed organic material, but other ε^* − FSC data pairs would imply different amounts of organic material ranging from 1 to 400 μg/g (with the maximum computed for the Concorde) for the same conversion fraction.

[59] The sulfur conversion fraction ε may depend on the engine and its state of operation. An engine chemistry model [*Tremmel and Schumann*, 1999] has been applied to compute ε for the thermodynamic conditions of the ATTAS and B737 engines during S5 and S6. The simulations (see Table 9) yield ε = 3.4–3.7% for the ATTAS engine and ε = 5.6–5.9% for the B737 (FSC = 100 μg/g in both cases). The computed values are within the range of measured values and show the same trend. The ε value is higher for the B737 engine than for the ATTAS because of the higher temperature and pressure behind the combustor. The model is applied with a prescribed exponential temperature and pressure decrease with time from combustor exit to engine exit fitted to engine data. With a different model and for

another engine (RB211-524B, pressure ratio 28) with even higher combustor exit pressure and temperature, *Starik et al.* [2002], see Table 9, compute ε up to 10%, and confirm the increase of ε with combustor exit pressure and temperature. This is further supported by an analysis of S^{VI} formation as a function of pressure and temperature in an equilibrium model [*Miake-Lye et al.*, 2001]. The factor 6 to 18 larger number of volatile particles larger 5 nm measured behind the A340 compared to the B707 (see Tables 6 and 8) also strongly suggests that ε is larger for the engines of the A340 with high pressure ratio compared to those of the older B707. The parameters of the Concorde engines (Olympus 593 Mk610) [*Deidewig*, 1998] are between those of the B737 engine and the RB 211 (pressure ratio 10.6, combustor exit pressure and temperature 9000 hPa and 1430 K, no bypass, overall propulsion efficiency 0.4 at cruise with Mach 2, and maximum smoke number at ground without afterburner of 26.4). As noted before, some of the fast aircraft chased by the Falcon were operated at reduced power settings. Hence the possibility of larger values for certain engines and operation conditions, with higher combustion pressure, cannot be excluded from the measurements.

[60] A conversion of ε yields an equivalent H_2SO_4-emission index $\varepsilon \times$ FSC $\times$ 98/32, where 98/32 is the molecular weight ratio for H_2SO_4 and S. For ε = 3% and a typical FSC = 400 μg/g one obtains an equivalent $EI(H_2SO_4)$ of 0.04 g H_2SO_4 kg^{-1}. This is comparable to the mean EI_{soot} of 0.04 g kg^{-1}, but markedly exceeds the EI_{soot} of 0.01 g kg^{-1} of modern jet engines. If the mean diameter of the volatile particles is 5 nm, and their density is close to 1.5 g cm^{-3}, then 10^{17} such particles per kilogram correspond to a mass EI of 0.01 g kg^{-1}. The inferred EI of volatile material is smaller than the $EI(H_2SO_4)$. Hence, for typical FSC values, sulfuric acid remains the most important condensed material in the plume besides water.

4.2. Soot and Volatile Particles

[61] Additionally, Table 8 lists the particle number emission indices (PEI) of total (volatile and nonvolatile) and soot particles derived from the various measurements. From the SULFUR experiments, values PEI = Δc N/ρ are derived from the measured particle concentrations Δc above background, air density ρ, and dilution factor N (mass of exhaust gases per unit mass of fuel burned), with N determined from measured tracers for fuel consumption (CO_2 concentration or temperature increase above ambient values; see Figure 2, for example), or from the observed plume diameter, or plume age and an empirical dilution law [*Schumann et al.*, 1998].

[62] The PEI for soot particles >50 nm identified in the Concorde plume with impactors [*Pueschel et al.*, 1997]
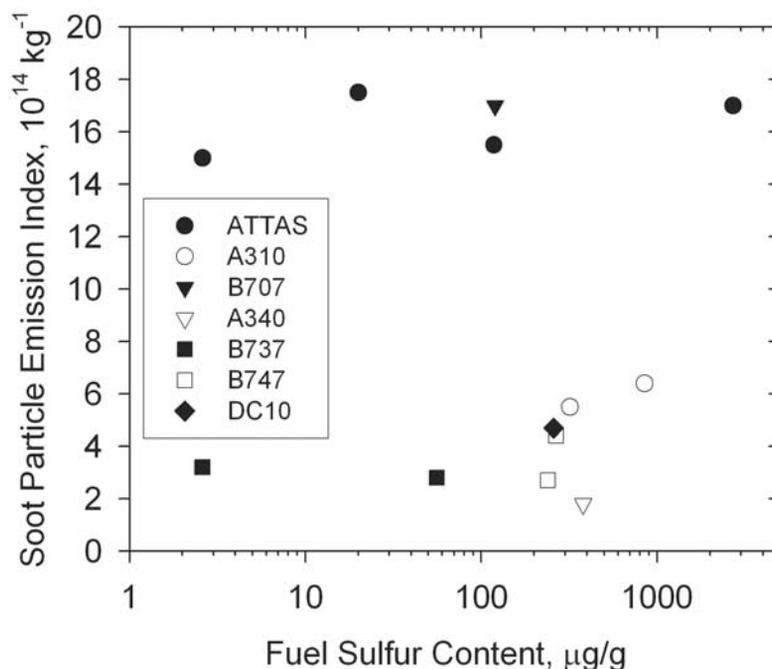
Figure 5. Soot particle number emission indices for particles >10 nm remaining after heating to 500 K versus fuel sulfur content. Data from S5, S6, S7, and POLINAT for various aircraft as listed. The ATTAS and B707 produce far more soot emissions than all other aircraft engines.

(computed from $EI_{soot} = \Delta c\ EI_{CO2} M_{air}/\{M_{CO2}\ \rho\ \Delta[CO_2]\}$ and the data from *Pueschel et al.* [1997]: $\Delta c = 0.21$ cm^{-3}, $EI_{CO2} = 3.16$, $M_{air} = 29$, $M_{CO2} = 44$, $\rho = 0.17$ kg m^{-3}, $\Delta[CO_2] = 0.34 \times 10^{-6}$) is 10^4 times smaller than the PEI of nonvolatile particles >9 nm counted with CPCs [*Fahey et al.*, 1995]; compatibility among both numbers and the reported soot mass emission index of 0.07 ± 0.05 g/kg [*Pueschel et al.*, 1997] would require a volume mean soot diameter <13 nm, which is not supported by other observations. The measurements obtained with CPCs behind several subsonic aircraft range from 2×10^{14} to 3×10^{15} kg^{-1}. Figure 5 shows that the soot EIs measured for the ATTAS and B737 do not depend on the FSC. The emissions vary mainly because of different engine technology, see Table 7, and show the same trend as the smoke number data of *ICAO* [1995] for lower than normal cruise power settings. The modern engines of the B737, B747, A310, A340, and DC10 have about a factor 10 smaller soot EIs than those of the older ATTAS and B707. For the particle size distribution of modern engines the aviation fleet of 1992 is estimated to emit 1.2×10^{15} kg^{-1} soot particles on average [*Petzold et al.*, 1999]. Slightly larger values measured in the North Atlantic flight corridor may include some volatile fractions [*Anderson et al.*, 1999a].

[63] For volatile particles the measurements generally show very large PEIs from less than 10^{15} to more than 10^{17} kg^{-1} increasing with decreasing cutoff diameter d and increasing FSC. Figure 6 summarizes the SULFUR results in noncontrail-forming plumes. The PEI for volatile particles larger than 5 nm increases by a factor of 10 for an increase of FSC from 2.6 to 2800 μg/g. Emissions of

particles larger 14 nm increase by a factor of 5 over this range. Further data are available from the SNIF III experiments, showing a maximum PEI of 8.7×10^{17} kg^{-1} particles larger 4 nm when burning fuel in an afterburner (possibly enhancing CI formation) of an F-16 fighter aircraft [*Anderson et al.*, 1999b]. Part of the variation in the PEI values is due to different engines and flight conditions. The PEI value of the B707 is lower than that of the A340 possibly because of more soot and hence more scavenging of volatile aerosols. The ATTAS is in between these technologies. Ultrafine CN increases measured with different methods relative to nitrogen oxides increases in minutes to 10 hours old aircraft plumes revealed PEI values between 10^{16} and 1.2×10^{17} kg^{-1} [*Schlager et al.*, 1997; *Anderson et al.*, 1999a].

[64] The data cannot be explained by the classical theory of binary homogeneous nucleation of H_2SO_4 with H_2O. This theory implies PEI values for $d > 3$ nm which are far below the PEI results measured for FSC <1000 μg/g and grow steeper than linear with FSC, different from what is observed [*Kärcher et al.*, 2000]. The data can be explained only when taking ion-induced nucleation and ion-enhanced coagulation into account. For matching the data the models [*Yu et al.*, 1998; *Kärcher et al.*, 2000] require an initial total ion concentration at engine exit of 4×10^8 cm^{-3} at temperature $T = 600$ K and pressure $p = 220$ hPa, or an ion EI of 2×10^{17} CIs per kg of fuel burned. These assumptions are approximately consistent with the number of ions measured at ground with a Gerdien condenser [*Arnold et al.*, 2000]. The models do not include cluster growth inside the engine before reaching the exit. The details of formation, dynamics, and particle nucleation for
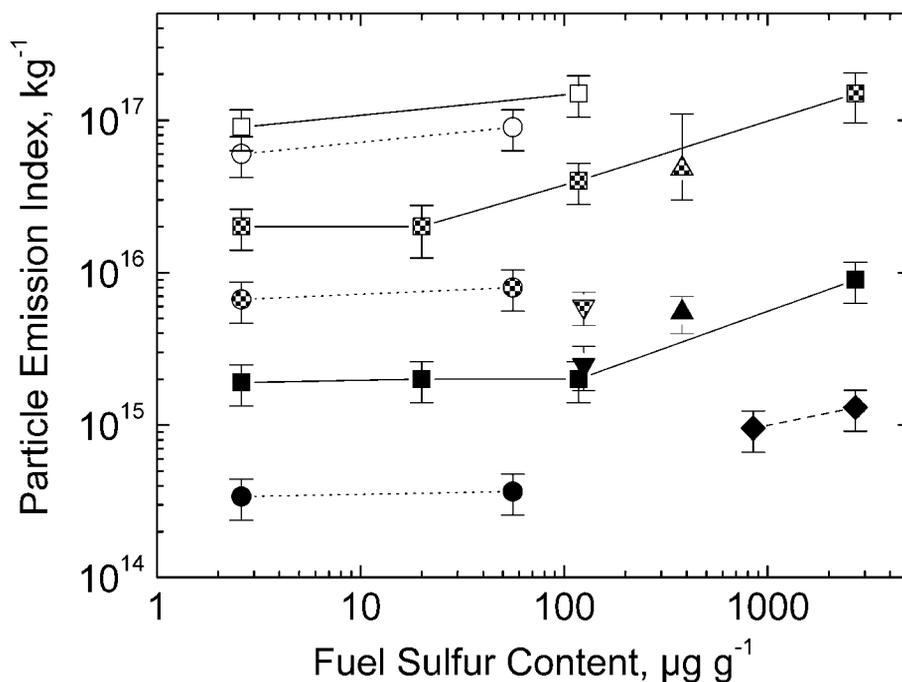
Figure 6. Emission index of the number of detectable volatile particles versus FSC in plumes without contrail formation, for various aircraft, lower detection limits d of particle diameters (open symbols: $d = 3$ nm; gray symbols: 5 nm; black symbols: 14 nm), and plume ages. ATTAS (squares) from S5, 7–9 s, and from S6, 0.5–7 s; B737 (circles) from S6, 0.4–0.6 s; A340 (upward pointing triangle) from S7, 0.5–1.5 s; and B707 (downward pointing triangle) from S7, 0.4–1.2 s. Note that the ATTAS values are higher than all others mainly because of the larger plume age.

ions, sulfuric acid, and condensable hydrocarbons from combustor exit to the nozzle exit have not yet been modeled.

[65] Much of the variation in volatile aerosols can be explained in terms of different size sensitivity of the CPC instruments, plume ages, and FSC values. *Kärcher et al.* [2000] provided an analytical model to explain the wide variance of observed PEIs in exhaust plumes. The model assumes that the number of CIs available determines the

number of nanometer-sized volatile particles detectable with CPCs in the exhaust plume. The amount of sulfuric acid (depending on FSC and the conversion fraction ε) and the amount of condensable organic matter control the size of the particles formed. Coagulation and dilution control the timescales of particle growth. Using this model, and the parameters listed in Table 10, the measured PEIs can be normalized to a given plume age (3 s) and cutoff size of the particle counters (5 nm), see Figure 7.

Table 10. Parameters Used for Normalizing the PEI to Fixed Cutoff Size and Plume Age

Aircraft	Project	FSC, μg g^{-1}	EI$_{OM}$, μg g^{-1}	ε, %	EI$_{CI}$, 10^{17} kg^{-1}	d, nm	t, s	PEI,[a] 10^{17} kg^{-1}
Concorde		230	70	15	5	9	960–3480	1.4
ATTAS	S5, S6	2700, 118, 20, 2.6	20–35	3–6	1.5–2	3–5	2–8	1.5, 0.36, 0.096, 0.14
B737	SNIF-II	800	20	2	1.5	4	25	0.87
F16	SNIF-III	146, 527, 942	1	0.5–1	3–4	4	0.5–16	0.46, 0.38, 1.14
DC8	SUCCESS	550	10	1	1.5	4	20–40	0.51
B747	POLINAT	240, 265	10	2	2	12	84, 88	0.26, 0.28
DC10	POLINAT	265	18	2	2	12	120	0.22
B737	S6	2.6, 56	30	5	3	3	0.15–0.4	0.29, 0.45
A340	S7	380	20	5.5 (4–12)	1.1 (0.9–1.8)	5	0.7	1.8
B707	S7	120	30	1	2	5	0.6	0.18

[a]Particle emission indices (PEIs) computed for plume age 3 s and cutoff diameter 5 nm (see Figure 7) for given fuel sulfur content (FSC) to fit volatile particle number concentrations measured with CPCs with cutoff diameter d at plume age t behind the Concorde [*Fahey et al.*, 1995] during SULFUR 5–7 [*Schröder et al.*, 1998, 2000b; *Brock et al.*, 2000; this work], SNIF-II, -III, and SUCCESS [*Anderson et al.*, 1998a, 1998b, 1999b], and POLINAT [*Schumann et al.*, 2000a], using values of EI of condensable organic matter (OM), fuel sulfur conversion fraction (ε), and EI of emitted CIs, for which the model fits the data optimally. Ranges are given for cases with several data. Data as in the work of *Kärcher et al.* [2000], with additions for B737 (S6), B707 (S7), and A340 (S7). The A340 values listed are best estimates; the values in parentheses cover a range of lower and upper estimates. The Concorde values fit the lowest measured PEI of 1.7×10^{17} kg^{-1} at plume ages of 960–3480 s; the model would match PEI values of at most 3.2×10^{17} kg^{-1} in the aged plume for EI$_{OM}$ = 100 μg/g, ε = 30%, and EI$_{CI}$ = 8×10^{17} kg^{-1}.
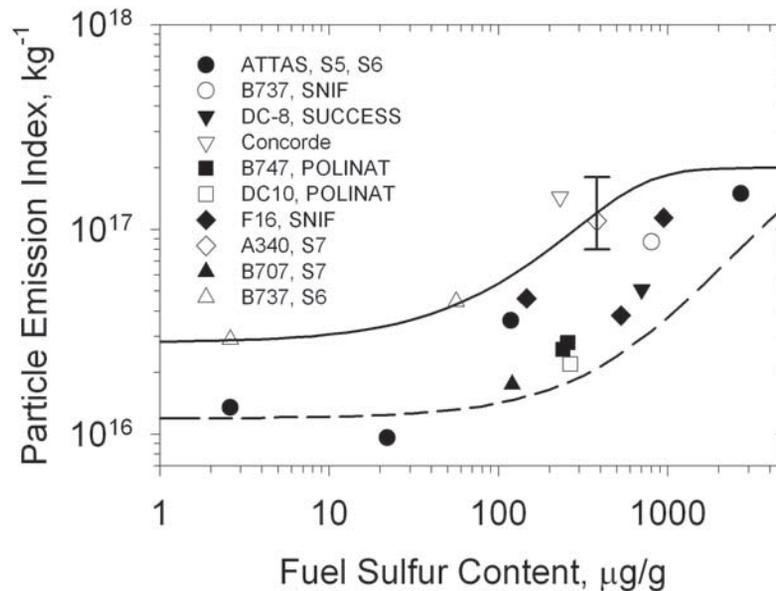
Figure 7. Particle number emission index (PEI) of detectable volatile particles in noncontrail plumes versus FSC from various measurements, normalized to plume age 3 s, CPC cutoff 5 nm, and various sulfur conversion fractions ε and emission indices of condensable organic matter, EI_{OM}, see Table 10, adjusted to approximate the measured concentrations as closely as possible. The result for the Concorde represents the value computed from the lower bound of the reported range of nonvolatile particle EIs [*Fahey et al.*, 1995]. The symbol and the error bar for the A340 represent the best estimate and the range derived from the particle concentrations measured. The curves emphasizing the trend of observed PEI with increasing FSC are model results at the same values of plume age, cutoff, and EI of CIs of 2×10^{17} kg^{-1}, and different EI_{OM} and ε values: 20 µg/g and 0.5% for dashed curve, and 30 µg/g and 8% for solid curve. From *Kärcher et al.* [2000] with additional data for the B737, A340, and B707 (S6 and S7).

The normalized PEIs scatter by a factor of 10, much less than the original data (compare Figure 6). Note the ambiguity in splitting the volatile mass into sulfuric acid and organic material (OM). A reduction of ε by $\Delta\varepsilon$ is equivalent to an increase in the EI of OM by $\Delta\varepsilon$ (98/32) FSC. For zero EI_{OM} the data would require maximum ε values of 25% to explain the lowest PEI data reported for the Concorde and 22% for the B737 with 56 µg/g FSC, and values even exceeding 100% for the lower FSC cases. Clearly, other condensable matter is required besides sulfuric acid to explain the observations. Most data (except the Concorde) are consistent with the model if the conversion fraction ε varies between 0.5 and about 10%, the amount of condensable organic matter between 1 and 30 µg/g, and the number of CIs emitted between 1 and 4×10^{17} kg^{-1}.

4.3. Particles in Contrails

[66] The number of volatile and nonvolatile (soot) particles within contrails differs from those in noncontrail (dry) plumes, see Figure 8. In the contrail environment with the interstitial inlet the CPCs count the aerosol not contained in contrail ice particles. The PEIs of the interstitial volatile particles are typically a factor 2–8 times smaller and show less trend with FSC compared to PEIs measured in dry plumes. In the young contrail the surface area of the ice particles (about 4×10^5 µm^2 cm^{-3} for the

B737 [*Schröder et al.*, 2000b]) is more than 100 times larger than the surface provided by aerosols in dry plumes (see Table 6). Hence a large fraction of the condensable gases, CIs, and volatile particles enters the ice particles [*Schröder et al.*, 1998, 2000b]. The early results from S2 (7 and 18 nm cutoff sizes) are consistent with the results from S4 to S7.

[67] The dependence on FSC of the number of ice particles formed is still uncertain from an observational point of view, see Figure 8. An increase of contrail crystal concentration with FSC was indicated by the color variations observed during S2 [*Schumann et al.*, 1996]. The color change observed was explained with a factor of 10 change in the number of ice particles formed for an FSC increase from 170 to 5500 µg/g [*Gierens and Schumann*, 1996]. A microphysical model computes a factor of 3 (increasing with decreasing ambient temperature) change in the number of ice crystals for such an FSC increase [*Kärcher et al.*, 1998a]. A far smaller increase in ice particle concentrations with FSC (factor 1.3 for 6 to 2800 µg/g) has been measured in the 10 s old contrails of the ATTAS during S4. However, as explained before, the S4 measurements provide only lower limit crystal concentrations [*Schröder et al.*, 2000a]. The actual values may be a factor of 10 larger than measured. Therefore the increase in ice crystal concentrations with FSC may be larger than measured during S4.
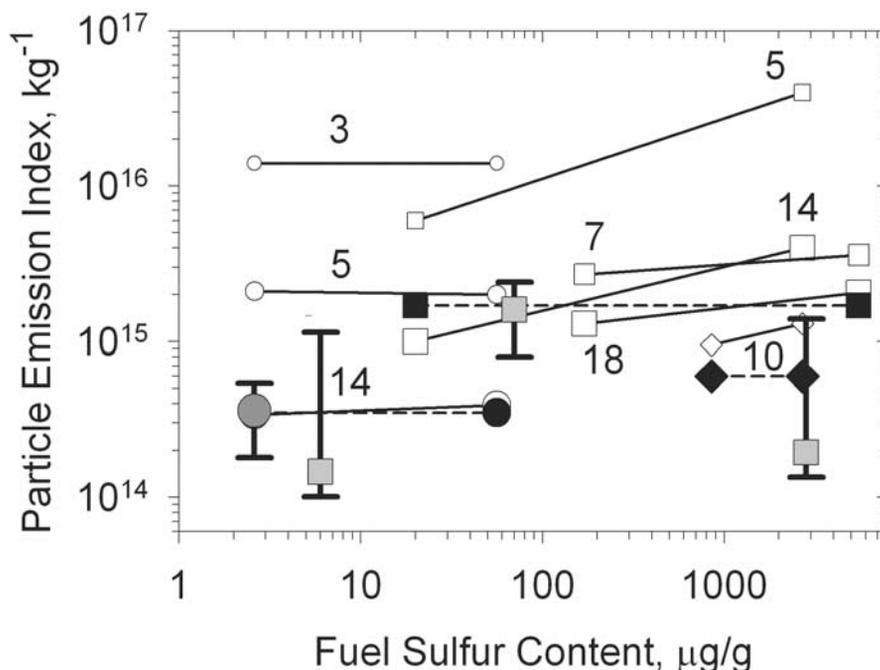
Figure 8. Emission index of detectable particle numbers in dissipating contrails for various aircraft and lower detection limits d of particle diameters versus FSC, behind the ATTAS (squares), B737 (circles), and A310 (diamonds). The open symbols with solid lines indicate data for volatile particles of various sizes in nanometers, as indicated; the symbol sizes are proportional to the particle diameters. The solid symbols with dashed lines approximate the mean soot particle emission indices measured for the three aircraft in noncontrail plumes. The gray symbols with error bars denote the number of ice particles formed per kilogram of fuel burned in contrails for the B737 (S6) and the ATTAS (S4 and S6). Data for B737 from S6 at 3, 5, and 14 nm and ice particles for 2.6 μg/g FSC at 0.4 s plume age; ATTAS (S2) 7 and 18 nm, 20 s; ATTAS (S4) ice particles for 6 and 2830 μg/g FSC, 10 s; ATTAS (S5) 5 and 14 nm, 20 s; ATTAS (S6) ice particles assigned to a mid FSC of 70 μg/g, 1 and 20 s; A310 (S4) 10 nm, 5 s.

[68] Ice particle concentration data were obtained with high accuracy during S6, with about 10 times higher concentration than in S4. Data are available from one flight behind the B737 for one low FSC value, and one flight behind the ATTAS burning alternatively fuels with FSC either 2.6 or 118 μg/g on the two engines. The differences in the ice crystal concentrations measured for the different FSC values are insignificant compared to the variability found along the flight track. Hence a trend with FSC cannot be detected from these data. The number of ice particles in the young contrail is larger for the ATTAS than for the B737 but about the same as the respective number of soot particles emitted in the dry plumes. Further, the number of contrail crystals corresponds roughly to the number of missing interstitial soot particles in the contrail. Hence most or at least many of the ice particles seem to be formed from soot particles for these cases with rather low FSC.

[69] Ice particle crystal concentrations were measured also behind 10 other aircraft in far older contrails (0.5 min to >30 min [Schröder et al., 2000a]). Using an empirical dilution law [Schumann et al., 1998], one computes from these data ice crystal "emission indices" (number per kilogram of fuel burned) of 1×10^{14} to 1×10^{15} kg^{-1}, without systematic trend with age, with variability partially due to different experimental conditions, and a range which fits to the range of measured soot PEI values.

5. Conclusions

[70] The series of SULFUR experiments provided observations and detailed measurements of the different types of aerosol and trace compounds within the exhaust plume and contrails of jet aircraft burning fuels with different fuel sulfur contents at cruise and at ground, as well as at plume ages from a few milliseconds to nearly a minute. The measured aerosol types include volatile and nonvolatile components in the size range from nanometers to micrometers, and the trace compounds include the major aerosol precursors sulfuric acid and chemiions (CIs). On the basis of these results and related model studies the questions raised at the beginning of these investigations may be answered as follows:

1. In regard to soot emissions, the ATTAS engines at cruise emit 0.1 g kg^{-1} mass of nonvolatile soot particles, which corresponds to 1.7×10^{15} particles per kg of burned fuel. The mass mean diameter of the soot mode is about 70 nm. The soot emissions are largest for the B707, emitting

0.5 g kg^{-1} of soot; the particles are even larger than for the ATTAS engines. More modern engines emit less soot by mass and number. The A340 and B737 engines emit 0.01 g kg^{-1}, corresponding to the emission of 0.25×10^{15} kg^{-1} particles per kilogram of burned fuel. The mass mean diameter of the exhaust soot aerosol is about 50 nm in the case of modern engines. The 1992 fleet average soot mass and number emission indices are about 0.04 g kg^{-1} and 1.2×10^{15} kg^{-1}, respectively.

2. With respect to the conversion fraction ε, the first direct measurements of sulfuric acid performed behind two aircraft have shown that the fraction of fuel sulfur converted to sulfuric acid is larger than 0.34% for the ATTAS and 3.3 ± 1.8% for a B737 aircraft. The aerosol volume measured implies $\varepsilon < 1.8$% for the ATTAS at high FSC, and the direct and aerosol-derived data imply $\varepsilon < 4.5$% at low FSC. Despite significant improvement, data on aerosol volume still have large uncertainty. The conversion fraction is smaller than implied by the amount of volatile particles measured because the particles contain condensable organic matter besides sulfuric acid and water. The aerosol measured in the plumes of various aircraft and the models suggests ε varies between 0.5 and 10% depending on the engine. According to model studies, ε grows with increasing pressure and temperature at combustor exit and hence may be larger for modern engines with larger pressure ratios than for older engines. Sulfuric acid is formed mainly inside the engine and in the young cooling exhaust jet and is then rapidly depleted from the gas phase within about a second as the plume age increases. Further measurements at higher FSC would enable one to determine ε with higher accuracy.

3. Concerning chemiions, the concentration of charged particles formed by combustion-induced chemiions (CIs) is high at engine exit. At ground the concentration is about 10^9 cm^{-3} at engine exit; i.e., of the order 10^{17} kg^{-1} of fuel burned. The positive and negative CIs are partly very massive (exceeding even 8500 amu), even for nearly sulfur-free fuel (FSC = 2 µg/g). Probably the growth of these CIs involves organic trace gases. Using fuel with FSC = 118 µg/g, a marked additional growth of negative but not of positive CIs is observed. This suggests a sulfur-containing molecule, e.g., H_2SO_4, to be at least in part responsible for the additional ion growth. Negative ions identified include the cluster ions HSO_4^- $(H_2SO_4)_n$, HSO_4^- $(H_2SO_4)_n(SO_3)_m$ ($n \leq 3$, $m = 0$, 1), and organic ions. Positive CIs mostly contain oxygen-containing organic compounds. The CI concentration decreases steeply with increasing plume age. In flight the CI composition and its change with plume age has been measured only under special conditions. A total negative ion concentration of $>5 \times 10^4$ cm^{-3} for a plume age of 1 s was inferred in one case, and an upper limit for positive ion concentrations of 3×10^6 cm^{-3} was derived at 3.6 s plume age from another case. CIs are now understood to be far more important for particle formation than some years ago. The formation of CIs in the combustor and their change on their way from the combustor through the engine as well as the details of particle formation are not yet understood.

4. The number of volatile particles with sizes >1.5 nm produced in aircraft plumes is of the order 2×10^{17} per kg of burned fuel, 100 to 1000 times larger than the number of soot particles emitted, and closely related to the number of CIs available initially. The size of the particles depends on plume age and the abundance of sulfuric acid and condensable organic matter, which are fuel- and engine-dependent. Our data suggest that for FSC exceeding about 100 µg/g, sulfuric acid seems to be the most important precursor of volatile aerosols formed in modern aircraft exhaust plumes. For lower FSC, organic trace gases, including oxygen-containing compounds, seem to be most important. The importance of volatile particles together with soot for cloud formation is not yet fully understood.

5. Contrails form when the mixture of exhaust gases and cold ambient air reaches liquid water saturation. At these conditions, liquid droplets form, mainly by condensation of H_2O on CN in the exhaust plume, which soon freeze to form ice particles. Incomplete dissipation of kinetic energy in the young jet, turbulent humidity fluctuations in the plume, and soot hydration before contrail onset may increase the threshold temperature for onset of contrail formation. However, the threshold temperature can be predicted to better than 1 K without taking such effects into account. Contrails form at higher ambient temperature for engines with higher overall propulsion efficiency. Both soot and volatile material contribute to nuclei for the formation of contrails and cirrus particles. However, changes in soot and FSC have little impact on the threshold temperature for contrail formation (less than 0.4 K). Contrails (with smaller optical thickness) would form even for zero particle emissions from the aircraft engines because of CN entrained into the exhaust plume from the ambient air. The aerosol remaining after contrail evaporation contains 2–8 times less particles but larger ones than formed in contrail-free plumes. From the few data available we find that the number of ice particles formed in young contrails is comparable to the number of soot particles and to increase by more than a factor of 1.3 for an increase in FSC from 6 to 2800 µg/g. The dependence of the number of ice particles on FSC (and ambient temperature) should be measured again with the improved FSSP-300 probe.

[71] The results show that fuel sulfur contributes to the amount of condensable volatile material in the exhaust plume, influences the size of volatile particles, and activates a larger part of soot particles to affect the number of ice particles formed. However, the effects of fuel sulfur on contrails are smaller than what has been expected before the series of SULFUR experiments was started and smaller than what was concluded from other experiments. The process of volatile particle formation is not controlled mainly by binary homogeneous nucleation of neutral clusters for which the number of particles would grow more than linear with the amount of FSC.

[72] The impact of soot and condensable matter on contrail particle formation is now relatively well understood. However, it is still not known which of the particles formed have the largest effect on cloudiness and chemistry and how large these effects are. This should be investigated in future projects. The emissions of engines are further investigated by our team in the EU project Measurement and Prediction of Emissions of Aerosols and Gaseous Precursors From Gas Turbine Engines (PARTEMIS), and the impact of aerosols on cirrus formation is now investigated in the EU project Interhemispheric Differences in Cirrus Properties from Anthropogenic Emissions (INCA;

see http://www.pa.op.dlr.de/INCA/). Moreover, an ongoing German project Partikel and Zirren (PAZI) deals with these questions (http://www.pa.op.dlr.de/pazi/).

References

Anderson, B. E., W. R. Cofer, D. R. Bagwell, J. W. Barrick, C. H. Hudgins, and C. E. Brunke, Airborne observations of aircraft aerosol emissions, 1, Total nonvolatile particle emission indices, *Geophys. Res. Lett.*, *25*, 1689–1692, 1998a.

Anderson, B. E., W. R. Cofer, J. W. Barrick, D. R. Bagwell, and C. H. Hudgins, Airborne observations of aircraft aerosol emissions, 2, Factors controlling volatile particle production, *Geophys. Res. Lett.*, *25*, 1693–1696, 1998b.

Anderson, B. E., et al., An assessment of aircraft as a source of particles to the upper troposphere, *Geophys. Res. Lett.*, *26*, 3069–3072, 1999a.

Anderson, B. E., W. R. Cofer III, and D. S. McDougal, Air Force F-16 aircraft engine aerosol emissions under cruise altitude conditions, *NASA Tech. Memo.*, TM-1999-209102, 1999b.

Andronache, C., and W. L. Chameides, Interactions between sulfur and soot emissions from aircraft and their role in contrail formation, 1, Nucleation, *J. Geophys. Res.*, *102*, 21,443–21,451, 1997.

Andronache, C., and W. L. Chameides, Interactions between sulfur and soot emissions from aircraft and their role in contrail formation, 2, Development, *J. Geophys. Res.*, *103*, 10,787–10,802, 1998.

Appleman, H., The formation of exhaust contrails by jet aircraft, *Bull. Am. Meteorol. Soc.*, *34*, 14–20, 1953.

Arnold, F., J. Scheid, T. Stilp, H. Schlager, and M. E. Reinhardt, Measurements of jet aircraft emissions at cruise altitude, 1, The odd-nitrogen gases NO, NO_2, HNO_2, and HNO_3, *Geophys. Res. Lett.*, *19*, 2421–2424, 1992.

Arnold, F., J. Schneider, M. Klemm, J. Scheid, T. Stilp, H. Schlager, P. Schulte, and M. E. Reinhardt, Mass spectrometric measurements of SO_2 and reactive nitrogen gases in exhaust plumes of commercial jet airliners at cruise altitude, *DLR-Mitt. 94-06*, pp. 323–328, Dtsch. Zentrum für Luft- und Raumfahrt, Cologne, Germany, 1994.

Arnold, F., T. Stilp, R. Busen, and U. Schumann, Jet engine exhaust chemiion measurements: Implications for gaseous SO_3 and H_2SO_4, *Atmos. Environ.*, *32*, 3073–3077, 1998a.

Arnold, F., K.-H. Wohlfrom, M. W. Klemm, J. Schneider, K. Gollinger, U. Schumann, and R. Busen, First gaseous ion composition measurements in the exhaust plume of a jet aircraft in flight: Implications for gaseous sulfuric acid, aerosols, and chemiions, *Geophys. Res. Lett.*, *25*, 2137–2140, 1998b.

Arnold, F., J. Curtius, B. Sierau, V. Bürger, R. Busen, and U. Schumann, Detection of massive negative chemiions in the exhaust plume of a jet aircraft in flight, *Geophys. Res. Lett.*, *26*, 1577–1580, 1999.

Arnold, F., A. Kiendler, V. Wiedemer, S. Aberle, T. Stilp, and R. Busen, Chemiion concentration measurements in jet engine exhaust at the ground: Implications for ion chemistry and aerosol formation in the wake of a jet aircraft, *Geophys. Res. Lett.*, *27*, 1723–1726, 2000.

Bögel, W., and R. Baumann, Test and calibration of the DLR Falcon wind measuring system by maneuvers, *J. Atmos. Oceanic Technol.*, *8*, 5–18, 1991.

Borrmann, S., B. Luo, and M. Mishenko, Application of the T-matrix method to the measurement of aspherical (ellipsoidal) particles with forward scattering optical particle counters, *J. Aerosol Sci.*, *31*, 789–799, 2000.

Brasseur, G. P., R. A. Cox, D. Hauglustaine, I. Isaksen, J. Lelieveld, D. H. Lister, R. Sausen, U. Schumann, A. Wahner, and P. Wiesen, European scientific assessment of the atmospheric effects of aircraft emissions, *Atmos. Environ.*, *32*, 2327–2422, 1998.

Brock, C. A., F. Schröder, B. Kärcher, A. Petzold, R. Busen, and M. Fiebig, Ultrafine particle size distributions measured in aircraft exhaust plumes, *J. Geophys. Res.*, *105*, 26,555–26,567, 2000.

Brown, R. C., R. C. Miake-Lye, M. R. Anderson, C. E. Kolb, and T. J. Resch, Aerosol dynamics in near-field aircraft plumes, *J. Geophys. Res.*, *101*, 22,939–22,953, 1996a.

Brown, R. C., M. R. Anderson, R. C. Miake-Lye, C. E. Kolb, A. A. Sorokin, and Y. I. Buriko, Aircraft exhaust sulfur emissions, *Geophys. Res. Lett.*, *23*, 3603–3606, 1996b.

Brown, R. C., R. C. Miake-Lye, M. R. Anderson, and C. E. Kolb, Aircraft sulfur emissions and the formation of visible contrails, *Geophys. Res. Lett.*, *24*, 385–388, 1997.

Busen, R., and A. L. Buck, A high-performance hygrometer for aircraft use: Description, installation, and flight data, *J. Atmos. Oceanic Technol.*, *12*, 73–84, 1995.

Busen, R., and U. Schumann, Visible contrail formation from fuels with different sulfur contents, *Geophys. Res. Lett.*, *22*, 1357–1360, 1995.

Cofer, W. R., III, B. E. Anderson, W. L. Winstead, and D. R. Bagwell, Calibration and demonstration of a condensation nuclei counting system for airborne measurements of aircraft exhausted particles, *Atmos. Environ.*, *32*, 169–177, 1998.

Cumpsty, N., *Jet Propulsion*, 281 pp., Cambridge Univ. Press, New York, 1997.

Curtius, J., and F. Arnold, Measurement of aerosol sulfuric acid, 1, Experimental setup, characterization, and calibration of a novel mass spectrometric system, *J. Geophys. Res.*, *106*, 31,965–31,974, 2001.

Curtius, J., B. Sierau, F. Arnold, R. Baumann, R. Busen, P. Schulte, and U. Schumann, First direct sulfuric acid detection in the exhaust plume of a jet aircraft in flight, *Geophys. Res. Lett.*, *25*, 923–926, 1998.

Curtius, J., F. Arnold, and P. Schulte, Sulfuric acid measurements in the exhaust plume of a jet aircraft in flight: Implications for the sulfuric acid formation efficiency, *Geophys. Res. Lett.*, *29*(7), 10.1029/2001GL013813, 2002.

Danilin, M. Y., J. M. Rodriguez, M. K. W. Ko, D. K. Weisenstein, R. C. Brown, R. C. Miake-Lye, and M. R. Anderson, Aerosol particle evolution in an aircraft wake: Implications for the high-speed civil transport fleet impact on ozone, *J. Geophys. Res.*, *102*, 21,453–21,463, 1997.

Deidewig, F., Ermittlung der Schadstoffemissionen im Unter- und Überschallflug, *DLR FB 98-10*, 163 pp., Dtsch. Zentrum für Luft- und Raumfahrt, Cologne, Germany, 1998.

Fahey, D. W., et al., Emission measurements of the Concorde supersonic aircraft in the lower stratosphere, *Science*, *270*, 70–74, 1995.

Fahey, D. W., U. Schumann, S. Ackerman, P. Artaxo, O. Boucher, M. Y. Danilin, B. Kärcher, P. Minnis, T. Nakajima, and O. B. Toon, Aviation-produced aerosols and cloudiness, in *Aviation and the Global Atmosphere*, edited by J. E. Penner et al., a special report of the Intergovernmental Panel on Climate Change (IPCC), chap. 3, pp. 65–120, Cambridge Univ. Press, New York, 1999.

Farago, Z., Fuel sulfur content, sulfur-oxide emission and corrosion in oil heating plants, *Combust. Sci. Technol.*, *79*, 73–96, 1991.

Frenzel, A., and F. Arnold, Sulfuric acid cluster ion formation by jet engines: Implications for sulfuric acid formation and nucleation, *DLR-Mitt. 94-06*, pp. 106–112, Dtsch. Zentrum für Luft- und Raumfahrt, Cologne, Germany, 1994.

Garnier, F., and A. Laverdant, Exhaust jet mixing and condensation effects in the near field of aircraft wakes, *Aerosp. Sci. Technol.*, *3*, 271–280, 1999.

Gerbig, C., D. Kley, A. Volz-Thomas, J. Kent, K. Dewey, and D. S. McKenna, Fast response resonance fluorescence CO measurements aboard the C-130: Instrument characterization and measurements made during the North Atlantic Regional Experiment 1993, *J. Geophys. Res.*, *101*, 29,229–29,238, 1996.

Gerz, T., and F. Holzäpfel, Wing-tip vortices, turbulence, and the distribution of emissions, *AIAA J.*, *37*, 1270–1276, 1999.

Gerz, T., T. Dürbeck, and P. Konopka, Transport and effective diffusion of aircraft emissions, *J. Geophys. Res.*, *103*, 25,905–25,913, 1998.

Gierens, K., and U. Schumann, Colors of contrails from fuels with different sulfur contents, *J. Geophys. Res.*, *101*, 16,731–16,736, 1996.

Gleitsmann, G., and R. Zellner, The effects of ambient temperature and relative humidity on particle formation in the jet regime of commercial aircraft: A modeling study, *Atmos. Environ.*, *32*, 3079–3087, 1998a.

Gleitsmann, G., and R. Zellner, A modeling study of the formation of cloud condensation nuclei in the jet regime of aircraft plumes, *J. Geophys. Res.*, *103*, 19,543–19,556, 1998b.

Gleitsmann, G., and R. Zellner, The aerosol dynamics of H_2O-H_2SO_4-HNO_3 mixtures in aircraft wakes: A modeling study, *Phys. Chem. Chem. Phys.*, *1*, 5503–5509, 1999.

Hagen, D. E., P. D. Whitefield, and H. Schlager, Particulate emissions in the exhaust plume from commercial jet aircraft under cruise conditions, *J. Geophys. Res.*, *101*, 19,551–19,557, 1996.

Hagen, D. E., P. Whitefield, J. Paladino, M. Trueblood, and H. Lilenfeld, Particulate sizing and emission indices for a jet engine exhaust sampled at cruise, *Geophys. Res. Lett.*, 25, 1681–1684, 1998.

Hallett, J., J. G. Hudson, and C. F. Rogers, Characterization of combustion aerosols for haze and cloud formation, *Aerosol Sci. Technol.*, 10, 70–83, 1990.

Hanisco, T. F., et al., The role of HO_x in supersonic and subsonic aircraft exhaust plumes, *Geophys. Res. Lett.*, 24, 65–68, 1997.

Harris, B. W., Conversion of sulfur dioxide to sulfur trioxide in gas turbine exhaust, *J. Eng. Gas Turbines Power*, 112, 585–589, 1990.

Haschberger, P., and E. Lindermeir, Observation of NO and NO_2 in the young plume of an aircraft jet engine, *Geophys. Res. Lett.*, 24, 1083–1086, 1997.

Haschberger, P., E. Lindermeir, and V. Tank, Airborne measurement of aircraft emissions using passive infrared FT spectroscopy, *DLR Mitt. 97-04*, pp. 89–98, Dtsch. Zentrum für Luft– und Raumfahrt, Oberpfaffenhofen, Germany, 1997.

Heland, J., and K. Schäfer, Determination of major combustion products in aircraft exhausts by FTIR emission spectroscopy, *Atmos. Environ.*, 32, 3067–3072, 1998.

Helten, M., H. G. J. Smit, D. Kley, J. Ovarlez, H. Schlager, R. Baumann, U. Schumann, P. Nedelec, and A. Marenco, In-flight intercomparison of MOZAIC and POLINAT water vapor measurements, *J. Geophys. Res.*, 104, 26,087–26,096, 1999.

Hofmann, D. J., Aircraft sulphur emissions, *Nature*, 349, 659, 1991.

Hofmann, D. J., and J. M. Rosen, Balloon observations of a particle layer injected by stratospheric aircraft at 23 km, *Geophys. Res. Lett.*, 5, 511–514, 1978.

Holzäpfel, F., T. Gerz, and R. Baumann, The turbulent decay of trailing vortex pairs in stably stratified environments, *Aerosp. Sci. Technol.*, 5, 95–108, 2001.

Hunter, S. C., Formation of SO_3 in gas turbines, *Trans. Am. Soc. Mech. Eng. J. Eng. Power*, 104, 44–51, 1982.

Hunton, D. E., et al., Chemical ionization mass spectrometric measurements of SO_2 emissions from jet engines in flight and test chamber operations, *J. Geophys. Res.*, 105, 26,841–26,855, 2000.

Intergovernmental Panel on Climate Change (IPCC), *Aviation and the Global Atmosphere*, edited by J. E. Penner et al., Cambridge Univ. Press, New York, 1999.

International Civil Aviation Organization (ICAO), Environmental protection: Aircraft engine emissions, vol. 2, 1st ed., annex 16 to the Convention on International Civil Aviation, 60 pp., Montreal, Quebec, Canada, 1981.

International Civil Aviation Organization (ICAO), Engine exhaust emissions data bank, *Doc. 9646-AN/943*, Montreal, Quebec, Canada, 1995. (Available at http://www.dera.gov.uk/aviation-emissions-databank.htm).

Jensen, E. J., O. B. Toon, S. Kinne, G. W. Sachse, B. E. Anderson, K. R. Chan, C. H. Twohy, B. Gandrud, A. Heymsfield, and R. C. Miake-Lye, Environmental conditions required for contrail formation and persistence, *J. Geophys. Res.*, 103, 3929–3936, 1998a.

Jensen, E. J., A. S. Ackerman, D. E. Stevens, O. B. Toon, and P. Minnis, Spreading and growth of contrails in a sheared environment, *J. Geophys. Res.*, 103, 31,557–31,568, 1998b.

Kärcher, B., Aircraft-generated aerosols and visible contrails, *Geophys. Res. Lett.*, 23, 1933–1936, 1996.

Kärcher, B., Physicochemistry of aircraft-generated liquid aerosols, soot, and ice particles, 1, Model description, *J. Geophys. Res.*, 103, 17,111–17,128, 1998a.

Kärcher, B., On the potential importance of sulfur-induced activation of soot particles in nascent jet aircraft exhaust plumes, *Atmos. Res.*, 46, 293–305, 1998b.

Kärcher, B., and D. W. Fahey, The role of sulfur emissions in volatile particle formation in jet aircraft exhaust plumes, *Geophys. Res. Lett.*, 24, 389–392, 1997.

Kärcher, B., T. Peter, and R. Ottmann, Contrail formation: Homogeneous nucleation of H_2SO_4/H_2O droplets, *Geophys. Res. Lett.*, 22, 1501–1504, 1995.

Kärcher, B., M. M. Hirschberg, and P. Fabian, Small-scale chemical evolution of aircraft exhaust species at cruising altitudes, *J. Geophys. Res.*, 101, 15,169–15,190, 1996a.

Kärcher, B., T. Peter, U. M. Biermann, and U. Schumann, The initial composition of jet condensation trails, *J. Atmos. Sci.*, 53, 3066–3083, 1996b.

Kärcher, B., R. Busen, A. Petzold, F. P. Schröder, U. Schumann, and E. J. Jensen, Physicochemistry of aircraft-generated liquid aerosols, soot, and ice particles, 2, Comparison with observations and sensitivity studies, *J. Geophys. Res.*, 103, 17,129–17,147, 1998a.

Kärcher, B., F. Yu, F. P. Schröder, and R. P. Turco, Ultrafine aerosol particles in aircraft plumes: Analysis of growth mechanisms, *Geophys. Res. Lett.*, 25, 2793–2796, 1998b.

Kärcher, B., R. P. Turco, F. Yu, M. Y. Danilin, D. K. Weisenstein, R. C. Miake-Lye, and R. Busen, A unified model for ultrafine aircraft particle emissions data, *J. Geophys. Res.*, 105, 29,379–29,386, 2000.

Kiendler, A., S. Aberle, and F. Arnold, Negative chemiions formed in jet fuel combustion: New insights from jet engine and laboratory measurements using a quadrupole ion trap mass spectrometer apparatus, *Atmos. Environ.*, 34, 2623–2632, 2000a.

Kiendler, A., S. Aberle, and F. Arnold, Positive ion chemistry in the exhaust plumes of an aircraft jet engine and a burner: Investigations with a quadrupole ion trap mass spectrometer, *Atmos. Environ.*, 34, 4787–4793, 2000b.

Kiendler, A., K.-H. Wohlfrom, S. Eichkorn, and F. Arnold, Measurement of chemiions in the exhaust plume of a jet engine: Total concentration, mass distribution and chemical composition, in *Proceedings of Aviation, Aerosols, Contrails and Cirrus Clouds, Seeheim, Germany, 10–12 July 2000*, edited by U. Schumann and G. T. Amanatidis, *EUR 19428*, pp. 132–135, Eur. Comm., Brussels, 2001.

Kolb, C. E., J. T. Jayne, D. R. Worsnop, M. J. Molina, R. F. Meads, and A. A. Viggiano, Gas phase reaction of sulfur trioxide with water vapor, *J. Am. Chem. Soc.*, 116, 10,314–10,315, 1994.

Konopka, P., and W. Vogelsberger, Köhler equation for finite systems: A simple estimation of possible condensation mechanisms in aircraft contrails, *J. Geophys. Res.*, 102, 16,057–16,064, 1997.

Konopka, P., U. Schumann, H. Schlager, D. E. Hagen, P. D. Whitefield, and J. Ovarlez, Particulate emissions of commercial jet aircraft under cruise conditions, *Rep. 93*, 13 pp., Inst. für Phys. der Atmos., Dtsch. Zentrum für Luft- und Raumfahrt, Oberpfaffenhofen, Germany, 1997.

Kuhn, M., A. Petzold, D. Baumgardner, and F. P. Schröder, Particle composition of a young condensation trail and of upper tropospheric aerosol, *Geophys. Res. Lett.*, 25, 2679–2682, 1998.

Lukachko, S. P., I. A. Waitz, R. C. Miake-Lye, R. C. Brown, and M. R. Anderson, Production of sulfate aerosol precursors in the turbine and exhaust nozzle of an aircraft engine, *J. Geophys. Res.*, 103, 16,159–16,174, 1998.

Miake-Lye, R. C., M. Martinez-Sanchez, R. C. Brown, and C. E. Kolb, Plume and wake dynamics, mixing and chemistry behind an HSCT aircraft, *J. Aircr.*, 30, 467–479, 1993.

Miake-Lye, R. C., R. C. Brown, M. R. Anderson, and C. E. Kolb, Calculations of condensation and chemistry in an aircraft contrail, *DLR Mitt. 94-06*, pp. 274–279, Dtsch. Zentrum für Luft- und Raumfahrt, Cologne, Germany, 1994.

Miake-Lye, R. C., et al., SO_x oxidation and volatile aerosol in aircraft exhaust plumes depend on fuel sulfur content, *Geophys. Res. Lett.*, 25, 1677–1680, 1998.

Miake-Lye, R. C., A. T. Chobot, S. P. Lukachko, R. C. Brown, J. Zhang, and I. A. Waitz, Simulation of post-combustion chemical evolution in gas turbine engines, in *Proceedings of Aviation, Aerosols, Contrails and Cirrus Clouds, Seeheim, Germany, 10–12 July 2000*, edited by U. Schumann and G. T. Amanatidis, *EUR 19428*, pp. 95–98, Eur. Comm., Brussels, 2001.

Paladino, J. D., D. E. Hagen, P. D. Whitefield, A. R. Hopkins, O. Schmidt, M. R. Wilson, and H. Schlager, Observations of particulates within the North Atlantic flight corridor: POLINAT 2, September–October 1997, *J. Geophys. Res.*, 105, 3719–3726, 2000.

Petzold, A., and A. Döpelheuer, Reexamination of black carbon mass emission indices of a jet engine, *Aerosol Sci. Technol.*, 29, 355–356, 1998.

Petzold, A., and F. P. Schröder, Jet engine exhaust aerosol characterization, *Aerosol Sci. Technol.*, 28, 62–76, 1998.

Petzold, A., et al., Near-field measurements on contrail properties from fuels with different sulfur content, *J. Geophys. Res.*, 102, 29,867–29,881, 1997.

Petzold, A., J. Ström, S. Ohlsson, and F. P. Schröder, Elemental composition and morphology of ice-crystal residual particles in cirrus clouds and contrails, *Atmos. Res.*, 49, 21–34, 1998.

Petzold, A., A. Döpelheuer, C. A. Brock, and F. P. Schröder, In situ observations and model calculations of black carbon emission by aircraft at cruise altitude, *J. Geophys. Res.*, 104, 22,171–22,181, 1999.

Pitchford, I. G., J. G. Hudson, and J. Hallett, Size and critical supersaturation for condensation of jet engine exhaust particles, *J. Geophys. Res.*, 96, 20,787–20,793, 1991.

Pueschel, R. F., K. A. Boering, S. Verma, S. D. Howard, G. V. Ferry, J. Goodman, D. A. Allen, and P. Hamill, Soot aerosol in the lower stratosphere: Pole-to-pole variability and contributions by aircraft, *J. Geophys. Res.*, 102, 13,113–13,118, 1997.

Pueschel, R. F., S. Verma, G. V. Ferry, S. D. Howard, D. Vay, S. Kinne, J. Goodman, and A. W. Strawa, Sulfuric acid and soot particle formation in aircraft exhaust, *Geophys. Res. Lett.*, 25, 1685–1688, 1998.

Rattigan, O. V., J. Boniface, E. Swartz, P. Davidovits, J. T. Jayne, C. E. Kolb, and D. R. Worsnop, Uptake of gas-phase SO_2 in aqueous sulfuric

acid: Oxidation by H_2O_2, O_3, and HONO, *J. Geophys. Res.*, *105*, 29,065–29,078, 2000.

Reiner, T., and F. Arnold, Laboratory flow reactor measurements of the reaction $SO_3 + H_2O + M \rightarrow H_2SO_4 + M$: Implications for gaseous H_2SO_4 and aerosol formation in the plume of jet aircraft, *Geophys. Res. Lett.*, *20*, 2659–2662, 1993.

Reiner, T., and F. Arnold, Laboratory investigations of gaseous sulfuric acid formation via $SO_3 + H_2O + M \rightarrow H_2SO_4 + M$: Measurement of the rate constant and product identification, *J. Chem. Phys.*, *101*, 7399–7407, 1994.

Schlager, H., P. Konopka, P. Schulte, U. Schumann, H. Ziereis, F. Arnold, M. Klemm, D. E. Hagen, P. D. Whitefield, and J. Ovarlez, In situ observations of air traffic emission signatures in the North Atlantic flight corridor, *J. Geophys. Res.*, *102*, 10,739–10,750, 1997.

Schmidt, E., Die Entstehung von Eisnebel aus den Auspuffgasen von Flugmotoren, in *Schriften der Deutschen Akademie der Luftfahrtforschung*, vol. 44, pp. 1–15, R. Oldenbourg, München, 1941.

Schröder, F. P., Vertikalverteilung und Neubildungsprozesse des Aerosols und partikelförmige Flugzeugemissionen in der freien Troposphäre und Tropopausenregion, doctoral thesis, 195 pp., Univ. Munich, Munich, Germany, 2000.

Schröder, F., and J. Ström, Aircraft measurements of submicrometer aerosol particles (>7 nm) in the midlatitude free troposphere and tropopause region, *Atmos. Res.*, *44*, 333–356, 1997.

Schröder, F. P., B. Kärcher, A. Petzold, R. Baumann, R. Busen, C. Hoell, and U. Schumann, Ultrafine aerosol particles in aircraft plumes: In situ observations, *Geophys. Res. Lett.*, *25*, 2789–2792, 1998.

Schröder, F., B. Kärcher, C. Duroure, J. Ström, A. Petzold, J.-F. Gayet, B. Strauss, P. Wendling, and S. Borrmann, On the transition of contrails into cirrus, *J. Atmos. Sci.*, *57*, 464–480, 2000a.

Schröder, F., C. A. Brock, R. Baumann, A. Petzold, R. Busen, P. Schulte, and M. Fiebig, In situ studies on volatile jet exhaust particle emissions: Impacts of fuel sulfur content and environmental conditions on nuclei mode aerosols, *J. Geophys. Res.*, *105*, 19,941–19,954, 2000b.

Schulte, P., H. Schlager, H. Ziereis, U. Schumann, S. L. Baughcum, and F. Deidewig, NO_x emission indices of subsonic long-range jet aircraft at cruise altitude: In situ measurements and predictions, *J. Geophys. Res.*, *102*, 21,431–21,442, 1997.

Schumann, U., On the effect of emissions from aircraft engines on the state of the atmosphere, *Ann. Geophys.*, *12*, 365–384, 1994.

Schumann, U., (Ed.), AERONOX–The impact of NO_x emissions from aircraft upon the atmosphere at flight altitudes 8–15 km, *Publ. EUR 16209 EN*, 471 pp., Off. for Publ. of the Eur. Comm., Brussels, 1995.

Schumann, U., On conditions for contrail formation from aircraft exhausts, *Meteorol. Z.*, *5*, 4–24, 1996a.

Schumann, U., Particle formation in jet aircraft exhausts and contrails for different sulfur- containing fuels, in *Nucleation and Atmospheric Aerosols 1996*, edited by M. Kulmala and P. E. Wagner, pp. 296–299, Pergamon, New York, 1996b.

Schumann, U., Influence of propulsion efficiency on contrail formation, *Aerosp. Sci. Technol.*, *4*, 391–401, 2000.

Schumann, U., J. Ström, R. Busen, R. Baumann, K. Gierens, M. Krautstrunk, F. P. Schröder, and J. Stingl, In situ observations of particles in jet aircraft exhausts and contrails for different sulfur-containing fuels, *J. Geophys. Res.*, *101*, 6853–6869, 1996.

Schumann, U., A. Dörnbrack, T. Dürbeck, and T. Gerz, Large-eddy simulation of turbulence in the free atmosphere and behind aircraft, *Fluid Dyn. Res.*, *20*, 1–10, 1997.

Schumann, U., H. Schlager, F. Arnold, R. Baumann, P. Haschberger, and O. Klemm, Dilution of aircraft exhaust plumes at cruise altitudes, *Atmos. Environ.*, *32*, 3097–3103, 1998.

Schumann, U., H. Schlager, F. Arnold, J. Ovarlez, H. Kelder, Ø. Hov, G. Hayman, I. S. A. Isaksen, J. Staehelin, and P. D. Whitefield, Pollution from aircraft emissions in the North Atlantic flight corridor: Overview on the POLINAT projects, *J. Geophys. Res.*, *105*, 3605–3631, 2000a.

Schumann, U., R. Busen, and M. Plohr, Experimental test of the influence of propulsion efficiency on contrail formation, *J. Aircr.*, *37*, 1083–1087, 2000b.

Schumann, U., J. Ström, F. Arnold, T. K. Berntsen, P. M. de F. Forster, J.-F. Gayet, and D. Hauglustaine, Aviation impact on atmospheric composition and climate, in *European Research in the Stratosphere 1996–2000*, chap. 7, *EUR 19867*, pp. 257–307, Eur. Comm., Brussels, 2001.

Slemr, F., H. Giehl, J. Slemr, R. Busen, P. Haschberger, and P. Schulte, Inflight measurements of aircraft nonmethane hydrocarbon emission indices, *Geophys. Res. Lett.*, *25*, 321–324, 1998.

Slemr, F., H. Giehl, M. Habram, J. Slemr, H. Schlager, P. Schulte, P. Haschberger, E. Lindemeir, A. Doepelheuer, and M. Plohr, In-flight measurements of aircraft CO and nonmethane hydrocarbon emission indices, *J. Geophys. Res.*, *106*, 7485–7494, 2001.

Sorokin, A., and P. Mirabel, Ion recombination in aircraft exhaust plumes, *Geophys. Res. Lett.*, *28*, 955–958, 2001.

Starik, A. M., A. M. Savel'ev, N. S. Titova, and U. Schumann, Modeling of sulfur gases and chemiions in aircraft engines, *Aerosp. Sci. Technol.*, *6*, 63–81, 2002.

Ström, J., R. Busen, M. Quante, B. Guillemet, P. R. A. Brown, and J. Heintzenberg, Pre-EUCREX intercomparison of airborne humidity measuring instruments, *J. Atmos. Oceanic Technol.*, *11*, 1392–1399, 1994.

Taleb, D. E., R. McGraw, and P. Mirabel, Time lag effects on the binary homogeneous nucleation of aerosols in the wake of an aircraft, *J. Geophys. Res.*, *102*, 12,885–12,890, 1997.

Thompson, H., B. Singh, and H. Schlager, Introduction to special section: Subsonic Assessment Ozone and Nitrogen Oxide Experiment (SONEX) and Pollution From Aircraft Emissions in the North Atlantic Flight Corridor (POLINAT 2), *J. Geophys. Res.*, *105*, 3595–3603, 2000.

Toon, O. B., and R. C. Miake-Lye, Subsonic Aircraft Contrail and Cloud Effects Special Study (SUCCESS), *Geophys. Res. Lett.*, *25*, 1109–1112, 1998.

Tremmel, H. G., and U. Schumann, Model simulations of fuel sulfur conversion efficiencies in an aircraft engine: Dependence on reaction rate constants and initial species mixing ratios, *Aerosp. Sci. Technol.*, *3*, 417–430, 1999.

Tremmel, H. G., H. Schlager, P. Konopka, P. Schulte, F. Arnold, M. Klemm, and B. Droste-Franke, Observations and model calculations of jet aircraft exhaust products and cruise altitude and inferred initial OH emissions, *J. Geophys. Res.*, *103*, 10,803–10,816, 1998.

Turco, R. P., O. B. Toon, J. B. Pollack, R. C. Whitten, I. G. Poppoff, and P. Hamill, Stratospheric aerosol modification by supersonic transport and space shuttle operations—Climatic implications, *J. Appl. Meteorol.*, *19*, 78–89, 1980.

Weisenstein, D. K., M. K. W. Ko, N. D. Sze, and J. M. Rodriguez, Potential impact of SO_2 emissions from stratospheric aircraft on ozone, *Geophys. Res. Lett.*, *23*, 161–164, 1996.

Whitefield, P. D., M. B. Trueblood, and D. E. Hagen, Size and hydration characteristics of laboratory simulated jet engine combustion aerosols, *Part. Sci. Technol.*, *11*, 25–36, 1993.

Wilson, J. C., J. H. Hyun, and E. D. Blackshear, The function and response of an improved stratospheric condensation nucleus counter, *J. Geophys. Res.*, *88*, 6781–6785, 1983.

Wohlfrom, K.-H., S. Eichkorn, F. Arnold, and P. Schulte, Massive positive and negative ions in the wake of a jet aircraft: Detection by a novel aircraft-based large ion mass spectrometer (LIOMAS), *Geophys. Res. Lett.*, *27*, 3853–3856, 2000.

Yu, F., and R. P. Turco, The role of ions in the formation and evolution of particles in aircraft plumes, *Geophys. Res. Lett.*, *24*, 927–930, 1997.

Yu, F., and R. P. Turco, Contrail formation and impacts on aerosol properties in aircraft plumes: Effects of fuel sulfur content, *Geophys. Res. Lett.*, *25*, 313–316, 1998a.

Yu, F., and R. P. Turco, The formation and evolution of aerosols in stratospheric aircraft plumes: Numerical simulations and comparisons with observations, *J. Geophys. Res.*, *103*, 25,915–25,934, 1998b.

Yu, F., and R. P. Turco, Ultrafine aerosol formation via ion-mediated nucleation, *Geophys. Res. Lett.*, *27*, 883–886, 2000.

Yu, F., R. P. Turco, B. Kärcher, and F. P. Schröder, On the mechanisms controlling the formation and properties of volatile particles in aircraft wakes, *Geophys. Res. Lett.*, *25*, 3839–3842, 1998.

Yu, F., R. P. Turco, and B. Kärcher, The possible role of organics in the formation and evolution of ultrafine aircraft particles, *J. Geophys. Res.*, *104*, 4079–4088, 1999.

Zaichik, L. I., A. B. Lebedev, A. M. Savel'ev, and A. M. Starik, Simulation of binary condensation of H_2O/H_2SO_4 in plumes of jet engines using Euler's method of fractions, *High Temp.*, *38*, 77–86, 2000.

Zhao, J., and R. P. Turco, Nucleation simulations in the wake of a jet aircraft in stratospheric flight, *J. Aerosol Sci.*, *26*, 779–795, 1995.

———————

F. Arnold, A. Kiendler, and K.-H. Wohlfrom, Bereich Atmosphärenphysik, Max-Planck-Institut für Kernphysik, Postfach 103980, 69117 Heidelberg, Germany. (frank.arnold@mpi-hd.mpg.de)

R. Busen, B. Kärcher, A. Petzold, H. Schlager, F. Schröder, and U. Schumann, (corresponding author), Institut für Physik der Atmosphäre, Deutsches Zentrum für Luft- und Raumfahrt, Oberpfaffenhofen, Postfach 1116, 82230 Wessling, Germany. (ulrich.schumann@dlr.de)

J. Curtius, Institute for Atmospheric Physics, Johannes Gutenberg University Mainz, Becherweg 21, D-55099 Mainz, Germany. (curtius@mail.uni-mainz.de)

Figure 1. (a) Photo of the Airbus A340 at cruise during S7 measuring about 70 m behind the right turbofans. The nose boom of the Falcon used for turbulence measurements is visible at the lower edge of the photo; (b) the Falcon with particle measurement systems below the wing and aerosol inlet at top of the fuselage during S4; (c) the ATTAS at cruise during S2 burning low (high) fuel sulfur content on left (right) engine; (d) the A340 and the B707, wing by wing, one with, the other without contrails during S7; (e) sample inlet behind the ATTAS engines at ground during S3; (f) Falcon measuring in the B707 plume 70 m behind the engines during S7.